NEW MEXICO STATE UNIVERSITY

LAS CRUCES, NEW MEXICO

CR-134137

A COMPUTER MODEL OF A PHASE-LOCK LOOP

By

Ralph Paul Shelton, B.S.E.E

A Thesis submitted to the Graduate School
in partial fulfillment of the requirements
for the Degree
Master of Science
in Electrical Engineering

Major Subject: Electrical Engineering

Partially Supported By

NASA Grant No. NGR-32-003-0

ENGINEERING EXPERIMENT STATION

NEW MEXICO STATE UNIVERSITY
LAS CRUCES, NEW MEXICO

A COMPUTER MODEL OF A PHASE-LOCK LOOP

By

Ralph Paul Shelton, B.S.E.E

A Thesis submitted to the Graduate School
in partial fulfillment of the requirements
for the Degree
Master of Science
in Electrical Engineering

Major Subject: Electrical Engineering

Partially Supported By
NASA Grant No. NGR-32-003-037

ENGINEERING EXPERIMENT STATION

I

"A Computer Model of a Phase-Lock Loop," a thesis prepared by Ralph Paul Shelton in partial fulfillment of the requirements for the degree of Master of Science in Electrical Engineering, has been approved and accepted by the following:

Dean of the Graduate School

Chairman of the Examining Committee

Date

Committee in charge:

Dr. Frank F. Carden, Chairman

Dr. Lonnie C. Ludeman

Dr. John D. Thomas

Dr. Richard H. Stark

ACKNOWLEDGMENT

The author is indebted to many for help and encouragement during the preparation of this thesis. Dr. Frank Carden, his advisor, has offered much encouragement and inspiration in the preparation of this thesis and throughout the author's graduate program. Mr. T. B. Hintz and Mr. W. P. Osborne have provided an excellent sounding board for many ideas and have offered much constructive criticism.

Special acknowledgment goes to my wife, Mary Kay, for typing the rough draft and preparing the illustrations as well as for her patient understanding during the preparation of this thesis.

Dr. Thomas Puckett of the New Mexico State University Computer Center was of great assistance in obtaining the large amount of computer time required for this thesis. Special thanks also go to Mr. A. L. Gilbert for providing timely experimental results confirming the model.

Recognition is due Mrs. R. C. Pearce for an excellent job in typing the final manuscript. Gratitude goes to the National Aeronautics and Space Administration for assistance in reproduction of this thesis.

VITA

[redacted]

September, 1963--Entered New Mexico State University, Las Cruces

January, 1964--Began Co-operative Educational Program, White Sands Missile Range, New Mexico

June, 1968--B.S. E.E., New Mexico State University, Las Cruces

January, 1968--Communications Research Group, New Mexico State University, Las Cruces

September 1968--Received NDEA Fellowship, New Mexico State University, Las Cruces

PROFESSIONAL AND HONORARY SOCIETIES

Eta Kappa Nu

Sigma Tau

Phi Kappa Phi

IEEE

ABSTRACT

A COMPUTER MODEL OF A PHASE-LOCK LOOP

BY

RALPH PAUL SHELTON, B.S. E.E.

Master of Science in Electrical Engineering

New Mexico State University

Las Cruces, New Mexico, 1970

Dr. Frank F. Carden, Chairman

This thesis presents a computer model of a PLL (phase-lock loop), preceded by a bandpass filter, which is valid when the bandwidth of the bandpass filter is of the same order of magnitude as the natural frequency of the PLL. This model is shown to agree with previously known results for the situation in which PLL natural frequency is much smaller than the bandpass filter bandwidth. New results for the PLL natural frequency equal to the bandpass filter bandwidth are presented.

The model presented herein is for a second order PLL operating with carrier plus noise as the input. However, it is shown that

extensions to higher order loops, and to the case of a modulated carrier are straightforward.

The new results presented give the cycle skipping rate of the PLL as a function of the input carrier to noise ratio when the PLL natural frequency is equal to the bandpass filter bandwidth. Preliminary results showing the variation of the output noise power and cycle skipping rates of the PLL as a function of the loop damping ratio for the PLL natural frequency equal to the bandpass filter bandwidth are also presented.

TABLE OF CONTENTS

LIST OF FIGURES

LIST OF SYMBOLS

SYMBOL		Page
ω_m	Radian frequency of modulating sine wave.	19
$\Delta\omega$	Frequency deviation	19
Δt	Basic time interval	20
$R(\tau)$	Autocorrelation function.	21
N_i	The ith gaussian random number.	21
τ	Dummy variable.	21
σ^2	Variance of the numbers, N_i	22
$S_n(\omega)$	Power spectrum of wide-band source.	23
ω	Radian frequency (general).	23
$H_c(s)$	Transfer function of fifth order Chebyshev filter . . .	24
b_i	Coefficients in $H_c(s)$.	24
σ_0	Variance of narrow-band noise	27
$H(\omega)$	General transfer function	27
R_R	Rice's impulse rate	28
ρ	Numerical IF CNR	28
β	IF bandwidth for ideal square spectrum.	30
r_i	Radius of gyration of noise from an ideal square filter.	30
r_c	Radius of gyration of noise from an ideal fifth order Chebyshev filter.	30
r_e	Empirical radius of gyration.	30
CNR	Carrier to noise ratio in the IF.	35
NP	Noise power into PLL.	35
$N_0/2$	Noise spectral density.	36
$S_0(\omega)$	Output power spectrum of noise generator.	36

SYMBOL		Page
G	Amplifier gain.	37
CNR_L	Carrier to noise ratio in the loop.	40
T_{ave}	Mean time to unlock	40
ANP	Average noise power out of PLL.	44

CHAPTER I

INTRODUCTION

The phase-lock loop is a device with a wide variety of applications in electronic systems. F. M. Gardner lists five representative applications in his book on the subject [1]. These are: a coherent transponder, frequency modulation demodulator, stabilizing oscillators, frequency multipliers and dividers, and pulse code modulation demodulators. In general, a phase-lock loop is useful whenever one needs a noiseless version of a noisy signal which is phase coherent with the original signal.

There is a large body of information concerning many specific uses of the PLL (phase-lock loop). However, no general solution, that is, one describing the function of the PLL for all situations, has been found for a loop of order higher than one. This is a direct result of the difficulties involved in solving the nonlinear differential equations describing these higher order loops. In spite of this difficulty, it is known that a second order PLL is superior to a first order PLL for many applications. Enough experimental data for second order loops has been obtained to allow such loops to function better than other known devices for some applications. One of the most glamorous applications of second order PLL has been in the communications systems for the Apollo program.

In the applications previously mentioned, the PLL is generally preceded by a bandpass filter. This bandpass filter is frequently

the IF (intermediate frequency amplifier) of a communications receiver. Thus, the input to the PLL is signal plus band-limited noise. This is the situation modeled in this thesis. Whenever the bandwidth of the IF is wide compared to the bandwidth of the PLL, one can ignore the bandpass characteristics of the IF and analyze the PLL as if the input were white noise plus the desired signal. This simplifies the analytical problem considerably. Most previous work with the second order PLL has been done for this case. An important computer model for the white noise case has been developed by Sanneman and Rowbotham [2]. This model was used to obtain the mean time to unlock for a carrier tracking PLL. It will be shown that the results of the computer model developed in this thesis agree with this mean time to unlock in the appropriate region. The model presented in this thesis is an improvement over previous work because it is valid when the input to the PLL cannot be considered to be white noise plus signal.

The model development begins with the derivation of a general baseband model for a PLL. This development, given in Chapter II, parallels that of Viterbi [3]. Chapter III specializes the model of Chapter II to the case with no noise. Computer simulation results which verify this specialization of the model are presented. Chapter IV is devoted to the development of a digital computer representation of the noise process used in the general development of Chapter II. Computer results showing the validity of this model are presented. Chapter V combines the results of Chapters III and IV

to give a computer implementation of the general model of Chapter II for the case when no modulation is present. The results of this model are compared to previously published work and some recently obtained experimental data to show the validity of the model as a whole. Chapter V also presents new results obtained with this model. Chapter VI gives conclusions and recommendations for future studies using this model and extensions thereof.

CHAPTER II

DEVELOPMENT OF THE GENERAL BASEBAND MODEL

2.1 Introduction

This chapter develops a baseband model for a phase-lock loop preceded by an IF. The development begins with the representation of a PLL in terms of ideal physical components. This representation, which is standard in the literature, is shown in figure 1 [1,2,3,7, 15]. The development of the baseband model parallels that of Viterbi [3]. The second section of this chapter specializes the model slightly. This specialization will simplify the explanation of the computer implementation given in Chapters III and V.

2.2 General Development

The development of the general model will begin with the mathematical models for the physical devices shown in figure 1.

The VCO (voltage controlled oscillator) is an oscillator for which the output frequency is directly proportional to the input voltage. In terms of instantaneous quantities:

$$\dot{\theta}_0(t) = K_1 v(t) \qquad (2.2.1)$$

where v is the input voltage and $\theta_0(t)$ is the phase of the output sinusoid.

The multiplier is modeled as an approximately ideal device, the departure from ideal being that the output is proportional to

the product of the inputs. That is, for inputs I_1 and I_2, and output Y, we have:

$$Y = K_2 I_1 I_2 \qquad (2.2.2)$$

K_2 is the multiplier gain. Since the multiplier is used as a phase detector in this system, K_2 is often referred to as the phase detector gain.

The linear filter is characterized by its impulse response, h(t). In the work following, it will be specialized to a second order filter. For the present, it will be most convenient to retain the general representation.

As mentioned in the Introduction, it is desired to model the PLL when it is preceded by an IF. In this case, the input may be represented as the sum of a signal plus noise.

$$x(t) = s(t) + n(t) \quad . \qquad (2.2.3)$$

The signal considered is a general angle modulated sinusoidal carrier.

$$s(t) = \sqrt{2}A \sin [\omega_0 t + \theta_i(t)] \quad . \qquad (2.2.4)$$

The noise is a narrow-band process because of the characteristics of the IF. S. O. Rice [4] has shown that such a noise process may be represented as:

$$n(t) = n_s(t)\sin\omega_0 t + n_c(t)\cos\omega_0 t \qquad (2.2.5)$$

where $n_s(t)$ and $n_c(t)$ are independent stochastic processes with baseband power spectra identical to that of the original process [9].

The output of the VCO is taken to be:

$$z(t) = \sqrt{2}B \cos [\omega_0 t + \theta_0(t)] \quad . \tag{2.2.6}$$

Now $R(t)$ can be calculated as follows:

$$R(t) = x(t)z(t)K_2 \quad . \tag{2.2.7}$$

By substitution (2.2.7) becomes:

$$R(t) = K_2[\sqrt{2}A \sin[\omega_0 t+\theta_i(t)]+n_s(t)\sin\omega_0 t + n_c(t)\cos\omega_0 t]$$

$$[\sqrt{2}B \cos\omega_0 t + \theta_0(t)] \quad . \tag{2.2.8}$$

This result is now simplified using the following trigonometric identities:

$$\sin(x)\cos(y) = \tfrac{1}{2}\sin(x+y) + \tfrac{1}{2}\sin(x+y) \tag{2.2.9}$$

$$\cos(x)\cos(y) = \tfrac{1}{2}\cos(x+y) + \tfrac{1}{2}\cos(x+y) \quad . \tag{2.2.10}$$

After applying the identities, (2.2.8) becomes:

$$R(t) = 2ABK_2[\tfrac{1}{2}\sin\{\omega_0 t + \theta_i(t) + \omega_0 t + \theta_0(t)\}$$

$$+ \tfrac{1}{2}\sin\{\omega_0 t + \theta_i(t) - \omega_0 t - \theta_0(t)\}]$$

$$+ \sqrt{2}BK_2 n_s(t)\{\tfrac{1}{2}\sin[\omega_0 t + \omega_0 t + \theta_0(t)] + \tfrac{1}{2}\sin[\omega_0 t - \omega_0 t - \theta_0(t)]\}$$

$$+ \sqrt{2}BK_2 n_c(t)\{\tfrac{1}{2}\cos[\omega_0 t + \omega_0 t + \theta_0(t)] + \tfrac{1}{2}\cos[\omega_0 t - \omega_0 t - \theta_0(t)]\}. \quad (2.2.11)$$

Next $y(t)$ is to be calculated. The calculation can be simplified by observing at the outset that the linear filter is a lowpass filter with a corner frequency much less than ω_0. This allows one to ignore the terms centered about $2\omega_0$ and write:

$$\underline{R}(t) = K_2 AB\sin[\theta_i(t) - \theta_0(t)] + \sqrt{\tfrac{1}{2}}K_2 B n_s(t)\sin[-\theta_0(t)]$$

$$+ \sqrt{\tfrac{1}{2}}K_2 B n_c(t)\cos[-\theta_0(t)] \quad . \quad (2.2.12)$$

With $\underline{R}(t)$ as the input to a linear filter with impulse response, $h(t)$, the output may be written as:

$$y(t) = \int_0^t \underline{R}(u)h(t-u)du \quad . \quad (2.2.13)$$

Now substituting $y(t)$ for ν in (2.2.1),

$$\dot{\theta}_0 = K_1 y(t) \quad (2.2.14)$$

or

$$y(t) = \dot{\theta}_0 / K_1 \quad . \quad (2.2.15)$$

Combining (2.2.12), (2.2.13), and (2.2.15) yields:

$$\dot{\theta}_0 = K_1K_2AB \int_0^t \sin[\theta_i(u) - \theta_0(u)]h(t-u)du$$

$$+\sqrt{\tfrac{1}{2}}K_1K_2B\int_0^t n_s(u)\sin[-\theta_0(u)]h(t-u)du$$

$$+\sqrt{\tfrac{1}{2}}K_1K_2B\int_0^t n_c(u)\cos[-\theta_0(u)]h(t-u)du \quad . \quad (2.2.16)$$

This equation is represented by the system shown in figure 2.

2.3 Some Specializations for Simplification

There are some specializations of the model, shown in figure 3, which simplify the implementation and retain much of the generality.

First, the product BK_1K_2 is a combination of loop parameters which may be considered as one parameter. Thus, the loop gain K is defined as:

$$K = BK_1K_2 \quad . \quad (2.3.1)$$

Second, note that the sine is an odd function and the cosine is an even function. Thus:

$$\sin(-\theta_0) = -\sin\theta_0 \quad (2.3.2)$$

$$\cos(-\theta_0) = \cos\theta_0 \quad . \quad (2.3.3)$$

Further if one considers only zero mean gaussian processes for $n(t)$, it is immaterial whether one writes $n(t)$ or $-n(t)$. Thus, both inverters in this portion of the loop may be omitted.

With the two previous simplifications one may model the system as shown in figure 3. The equation describing the system then becomes:

$$\dot{\theta}_0 = AK\int_0^t \sin[\theta_i(u) - \theta_0(u)]h(t-u)du$$

$$+\sqrt{\tfrac{1}{2}}K\int_0^t n_s(u)\sin\theta_0(u)h(t-u)du$$

$$+\sqrt{\tfrac{1}{2}}K\int_0^t n_c(u)\cos\theta_0(u)h(t-u)du \quad . \qquad (2.3.4)$$

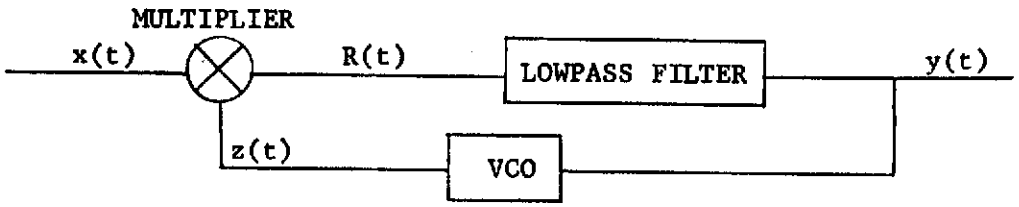

The PLL in Terms of Physical Components

figure 1

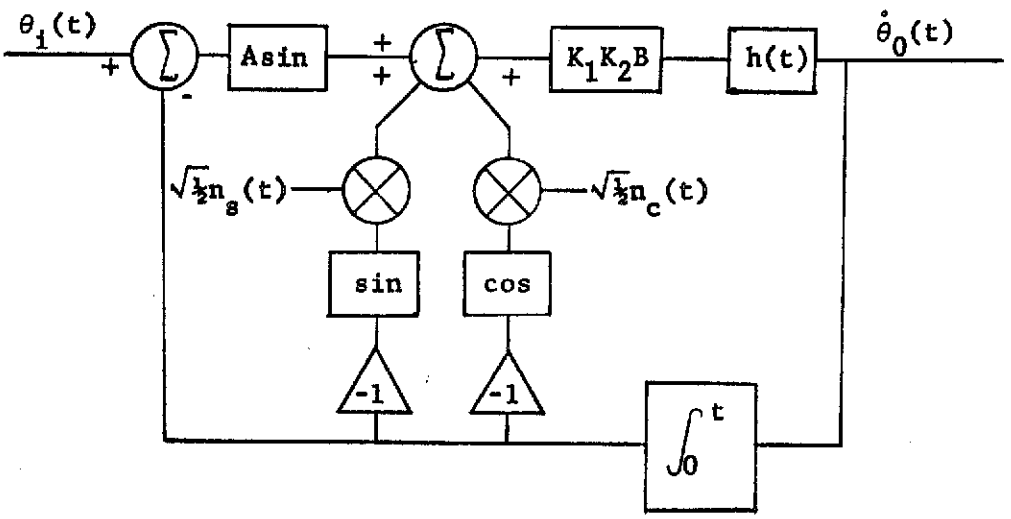

Block Diagram of the General Baseband Model

figure 2

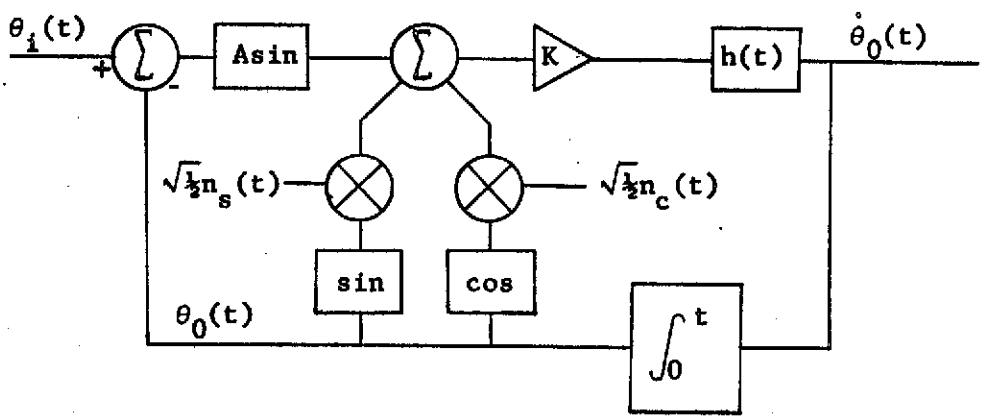

Simplified Block Diagram of the Baseband Model

figure 3

CHAPTER III

DETERMINISTIC MODEL VERIFICATION

3.1 Introduction

In this chapter the general model of Chapter II will be specialized to a second order phase-lock loop. Further, only the deterministic response will be considered. The implementation of the deterministic model will be discussed in detail. Finally, the results obtained with this implementation will be shown to agree with previously published results for the deterministic response of a second order PLL.

3.2 Deterministic Model

A model for a phase-lock loop with deterministic inputs may be derived, beginning with (2.3.4). If $n_s(t)$ and $n_c(t)$ are set to zero in (2.3.4) one obtains:

$$\dot{\theta}_0 = AK \int_0^t \sin[\theta_i(u) - \theta_0(u)]h(t-u)du \quad . \quad (3.2.1)$$

This equation is represented in block diagram form in figure 4. Figure 4 may also be viewed as being derived directly from figure 3 with $n_s(t)$ and $n_c(t)$ set to zero.

This is a standard representation for the deterministic base-band model, and similar developments may be found in books by Viterbi [3] and Gardner [1].

All results presented in this thesis are based on the following specializations. First, the carrier amplitude A is assumed fixed at unity. The filter, represented in general by $h(t)$ in (3.2.1), was specialized to a filter of the form:

$$H_f(s) = 1 + \frac{a}{s} \qquad (3.2.2)$$

in terms of the s-domain transfer function.

Now rewriting (3.2.1) in s-domain notation, substituting (3.2.2) for $H(s)$, and setting $A = 1$, one obtains:

$$s\theta_0(s) = K[\sin\{\theta_i(s) - \theta_0(s)\}]\ [1 + \frac{a}{s}] \quad . \qquad (3.2.3)$$

Thus, (3.2.3) is represented in block diagram form in figure 5.

Figure 5 represents the way in which the deterministic PLL model was implemented. A few more steps are necessary to represent this model in terms of the parameters most commonly used in the literature. The first step in this procedure will be to assume $\theta_i \approx \theta_0$ and hence $\sin(\theta_i - \theta_0) \approx \theta_i - \theta_0$. Thus, (3.2.3) now becomes:

$$s\theta_0(s) = K[\theta_i(s) - \theta_0(s)]\ [1 + \frac{a}{s}] \quad . \qquad (3.2.4)$$

This may be rewritten as:

$$\frac{\theta_0(s)}{\theta_i(s)} = \frac{sK + aK}{s^2 + Ks + aK} \quad . \qquad (3.2.5)$$

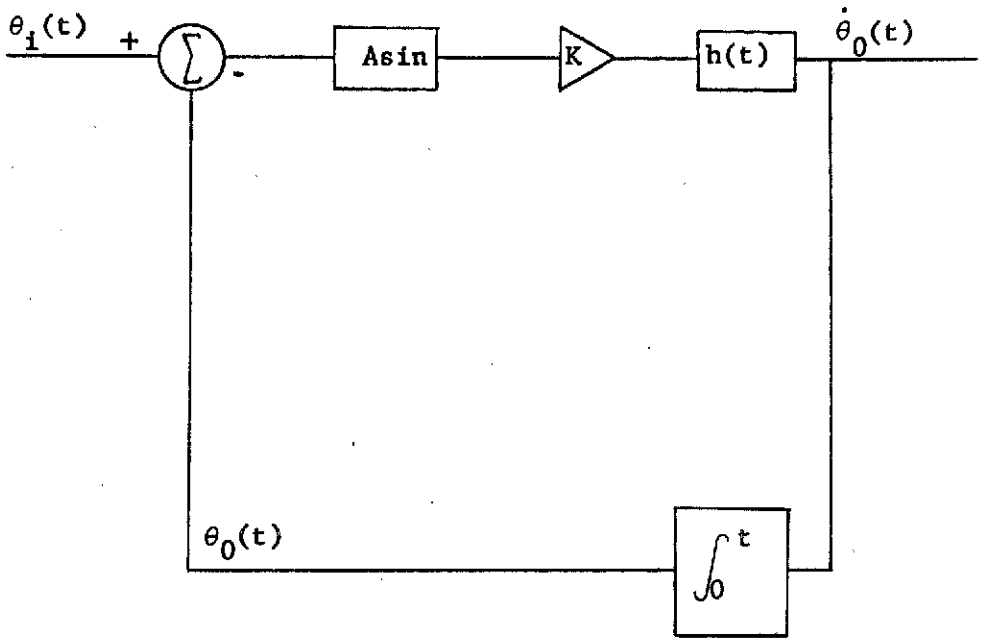

General Deterministic PLL Model

figure 4

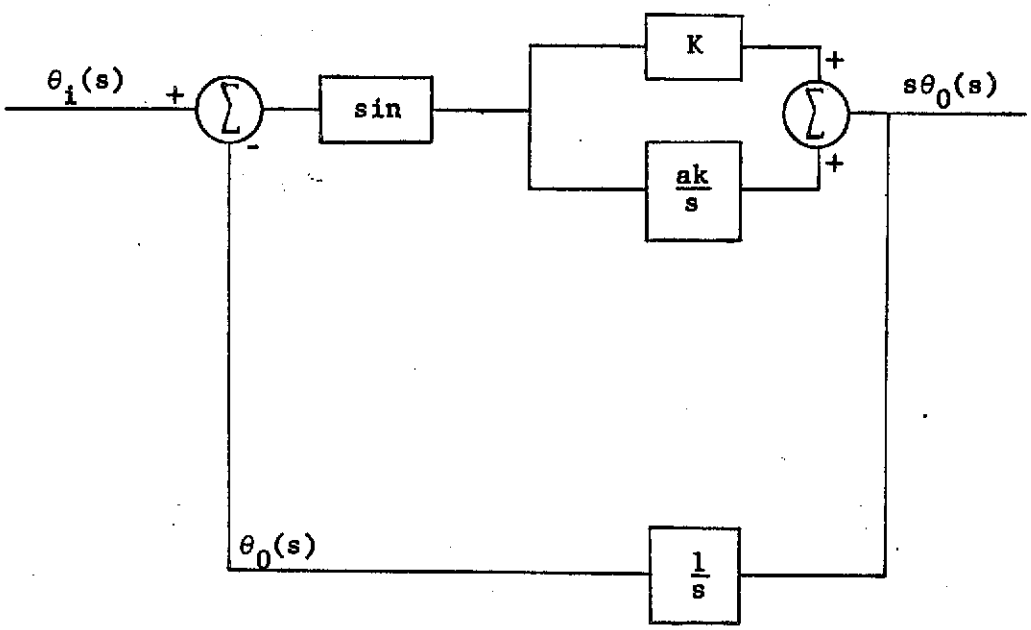

Deterministic Second Order PLL Model

figure 5

Transfer functions with second order denominators commonly occur in elementary closed loop systems theory. The response of such systems is characterized by two parameters. These are normally referred to as zeta (ζ), the damping ratio, and ω_n, the system natural frequency. The denominator of the transfer function is normally written as:

$$s^2 + 2\zeta\omega_n s + \omega_n^2 \quad . \tag{3.2.6}$$

Thus, for the second order PLL:

$$K = 2\zeta\omega_n \tag{3.2.7}$$

$$aK = \omega_n^2 \quad . \tag{3.2.8}$$

In terms of these parameters, (3.2.4) can be rewritten as:

$$s\theta_0(s) = [\theta_i(s) - \theta_0(s)] \left[\omega_n^2 + \frac{2\zeta\omega_n}{s}\right] \tag{3.2.9}$$

and figure 5 can be redrawn as shown in figure 6.

The form of the model depicted in figure 6 was used for deterministic studies of the second order PLL.

3.3 Computer Implementation

It will be most convenient to describe the digital computer implementation of the model with reference to a block diagram. Figure 6 represents the system simulated. Since the simulation is in the time-domain, figure 6 is redrawn, using time-domain notation, as figure 7.

The digital computer simulation was derived directly from this block diagram. The operations indicated on the diagram were performed over discrete blocks of time. A computer program for step response and a block diagram similar to figure 7 annotated with the computer program variables are included in Appendix A.

Three important points with respect to the simulation will now be considered. First, the basic simulation rate will be considered; second, the integration method; and third, the determination of the input.

The basic simulation rate was empirically determined by starting at a very high sample rate, with a step input to the system, and then lowering the sample rate until some degradation was observed. In this context degradation means a change in the output was observed. This is based on the assumption that as one increases the sample rate a better representation of the system is obtained. The sample rate was then set at a slightly higher rate. This rate may also be viewed as the integration interval for it is the basic time segment for the numerical integration technique. For all results presented in this thesis, the sample rate was 20 samples per second.

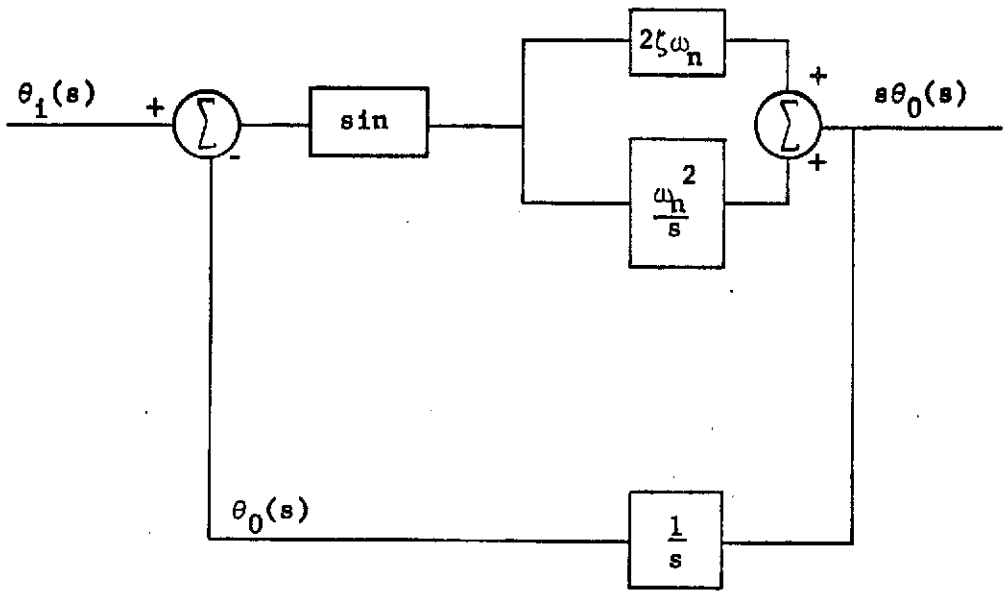

s-domain Block Diagram of Deterministic Model

figure 6

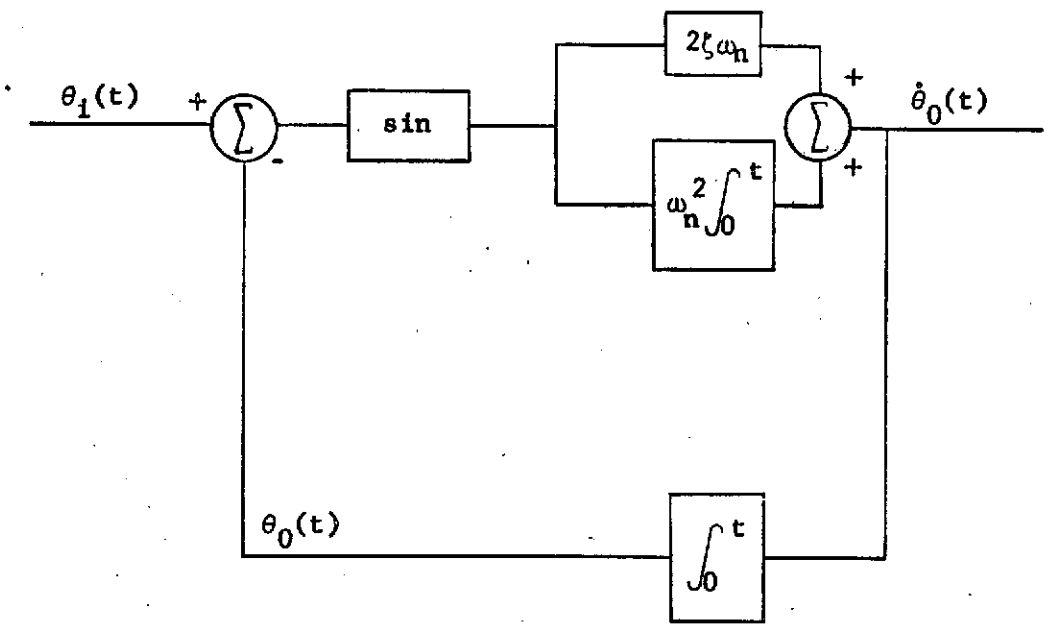

Time-domain Block Diagram of Deterministic Model

figure 7

The integration method used was suggested by F. E. Nixon [5]. It was chosen simply because it is easy to implement. This method, called the weighted average method, averages the derivative of the integral over two successive time intervals and uses this value as the rate of change of the integral. The use of an average derivative is thought to add stability to the numerical technique. However, no detailed analysis of the technique was made. The integration method is not claimed to be optimal but merely sufficient for the needs of the work presented here. However, some preliminary comparisons indicate this method is much faster on the digital computer than more commonly used differential equation solution methods such as the Runge-Kutta method. A study to determine which of the many available numerical integration techniques is optimum in some particular sense could be a topic worthy of a thesis in itself.

The input to the model just developed is the phase of the input carrier. It should be noted that references to the type of modulation refer to frequency modulation. Thus, a step input is a step in frequency which is a ramp in phase, and a cosine modulation appears at $\theta_i(t)$ as a sine. This is an important point to remember when interpreting the programs included.

3.4 Verification of Deterministic Response

One of the primary areas of interest in this investigation is the cycle skipping behavior of the phase-lock loop. Thus, the investigations for deterministic inputs were designed to show that

the phase-locked loop, as modeled in this presentation, loses lock for the same deterministic inputs as in previous studies.

The results for a frequency modulation step are shown in figure 8. The heavy lines are from reference [7]. The points shown with circles were determined with the model described earlier in this chapter.

Figure 9 shows regions of stability and instability as presented in reference [6] for frequency modulation by a single sine wave. Points determined using the model of this chapter are also shown in figure 9. Circles represent stable points and triangles represent unstable points.

The agreement shown by the figures is very good. It should be noted that reference [6] mentioned that the line shown in figure 9 does not represent a sharply-defined boundary. Further, the center point in each group of three points had rather large phase errors (greater than $\frac{\pi}{2}$). However, the output was still a reasonable approximation of a sine wave.

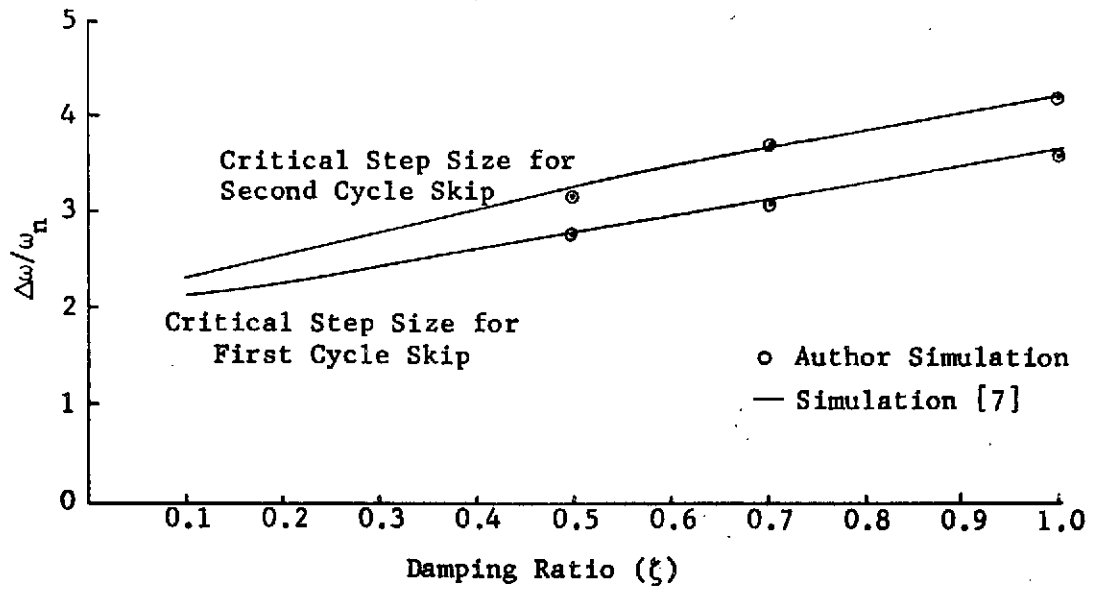

Verification of Deterministic Model for Step Input

figure 8

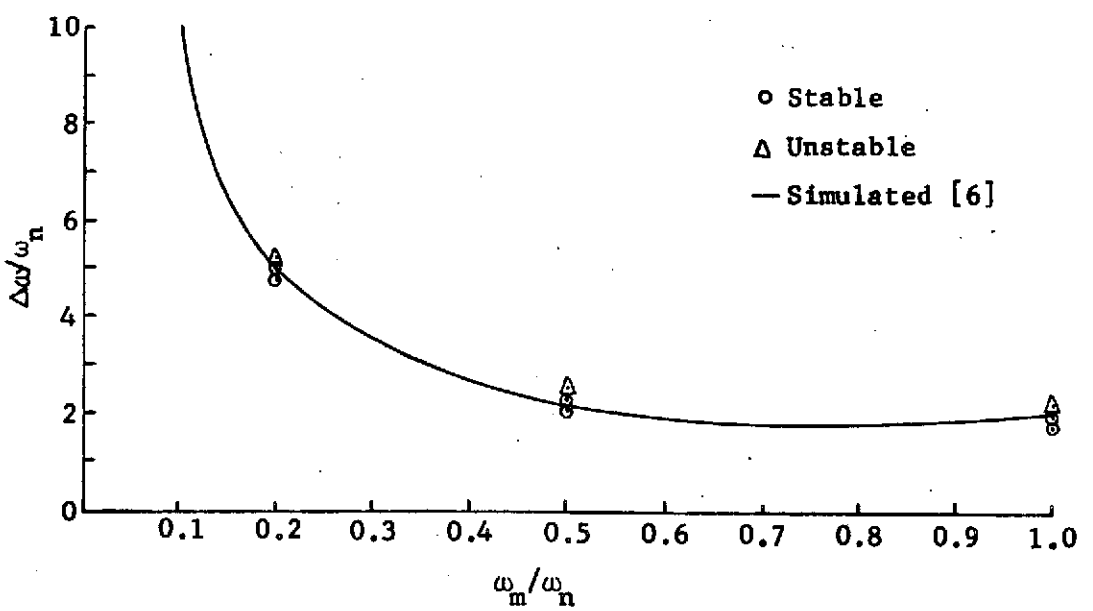

Verification of Deterministic Model for Sine Input

figure 9

CHAPTER IV

THE NOISE MODEL

4.1 Introduction

In this chapter a model for the narrow-band noise processes, $n_s(t)$ and $n_c(t)$ of Chapter II, will be developed. The model is specifically designed for easy implementation on a digital computer. The model begins with a wide-band noise source which is described in section 4.2. The wide-band noise from this source is passed through a filter with a passband narrow compared to the spectrum of the noise source. Thus the output of the filter is the same as if the input were white noise. The filter is described in section 4.3. The results of tests on the noise model as a whole are presented in section 4.4.

4.2 The Wide-band Noise Source

The fundamental noise source was a gaussian random number generator. The output numbers from this source were independent with a gaussian probability distribution about a zero mean. This random number generator is described in Appendix B. Each number from the random number generator was taken to represent the amplitude of a time function for a period of Δt seconds. This time function is illustrated in figure 10.

Now the power spectrum of the process will be found. This is the Fourier transform of the autocorrelation function. For the

following calculations the process will be assumed ergodic. The ergodicity of the process will be used to calculate the autocorrelation function. This development follows that of Lee [8].

For an ergodic process, x(t), the autocorrelation function may be written as:

$$R(\tau) = \lim_{T\to\infty} \int_{-T}^{T} x(t)x(t+\tau)dt \quad . \qquad (4.2.1)$$

This integral will be evaluated over two regions and the results combined to give $R(\tau)$ for all τ .

First, consider the region where $|\tau| > \Delta t$. For this region, $x(t)$ and $x(t + \tau)$ are independent. Since the process is generated with zero mean, the average of the product of $x(t)$ and $x(t+\tau)$ will be zero for this region. Hence:

$$R(\tau) = 0 \qquad |\tau| > \Delta t \quad . \qquad (4.2.2)$$

To evaluate $R(\tau)$ for $|\tau| < \Delta t$ it will be most advantageous to first consider a single region of width Δt. The functions $x(t)$ and $x(t+\tau)$ are illustrated for a typical region of this type in figure 11. The number N_i is the output of the random number generator in the interval Δt . From the illustration the integral of the desired product in the interval Δt can be viewed as an area and written as:

$$\int_{t_1}^{t_1+\Delta t} x(t)x(t+\tau)dt = N_i N_{i-1}\tau + N_i^2 (\Delta t - \tau) \quad . \qquad (4.2.3)$$

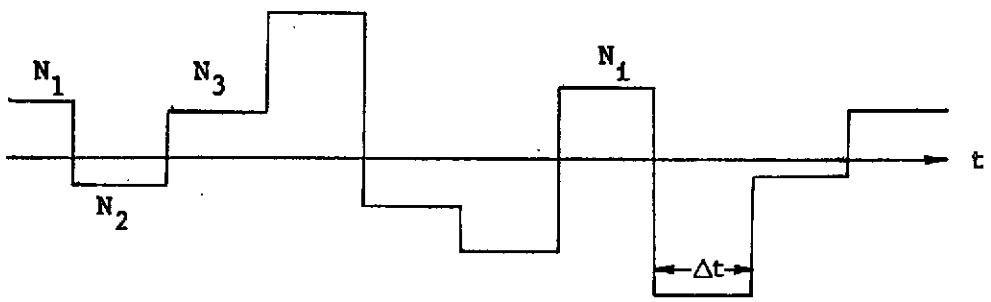

Typical Time Series of Wide-band Noise

figure 10

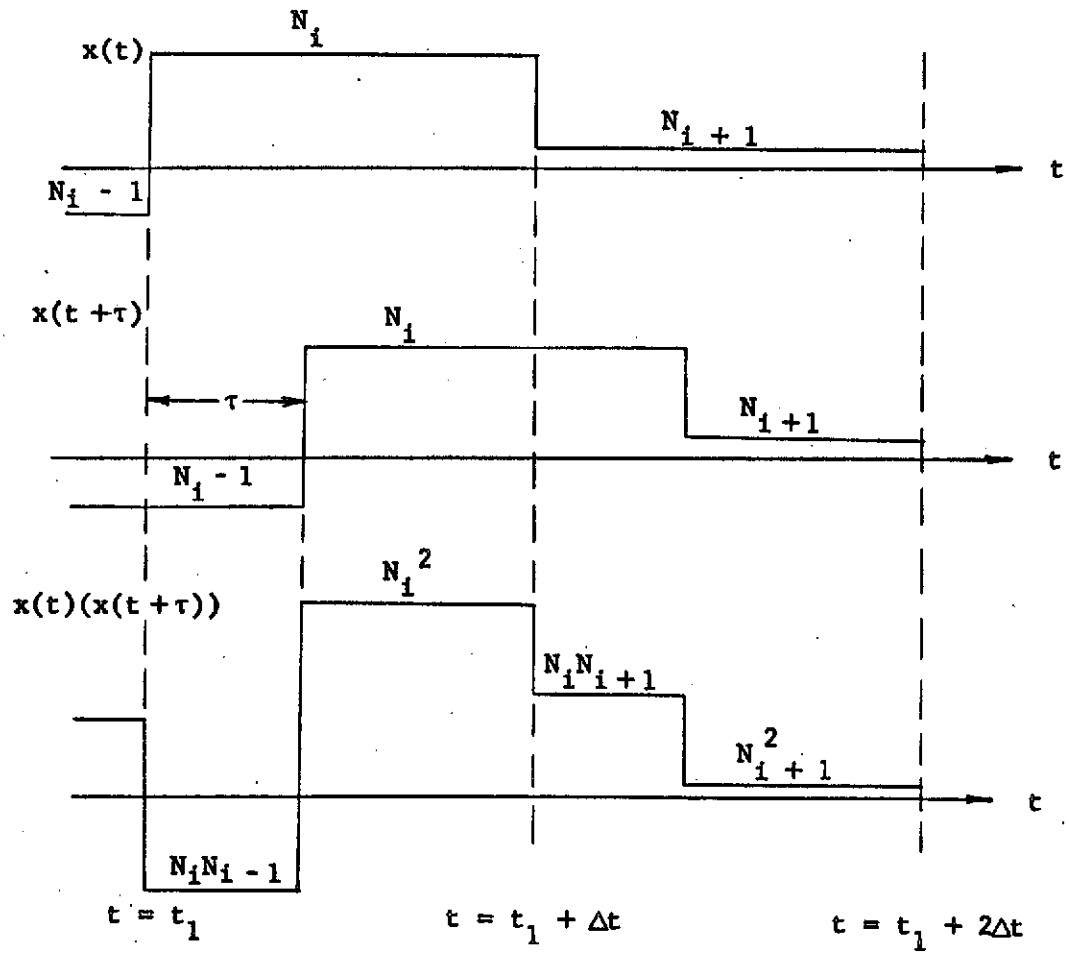

Typical Interval for Calculation of Autocorrelation Function

figure 11

Over this interval the normalizing factor multiplying the integral is simply $\frac{1}{\Delta t}$. Hence, for the interval, the integral is:

$$[N_i N_{i-1}\tau]/\Delta t + [N_i{}^2(\Delta t \quad \tau)]/\Delta t \quad . \qquad (4.2.4)$$

The entire integral corresponds to averaging over all such intervals. The average of $N_i N_{i+1}$ is zero from the way in which the N_i are generated. Further, the average of $N_i{}^2$ is simply the variance, σ^2 , of the random number generator. Hence, applying the same arguments to negative shifts:

$$R(\tau) = \sigma^2(\Delta t - |\tau|)/\Delta t \qquad |\tau|<\Delta t \quad . \qquad (4.2.5)$$

This result is shown pictorially in figure 12.

Now for the power spectrum, $S_n(\omega)$, the Fourier transform of $R(\tau)$ is taken.

$$S_n(\omega) = \int_{-\infty}^{\infty} R(\tau) e^{-j\omega\tau} d\tau \qquad (4.2.6)$$

for this $R(\tau)$:

$$S_n(\omega) = \int_{\Delta t}^{0} \frac{\sigma^2(\Delta t + \tau)}{\Delta t} e^{-j\omega\tau} d\tau + \int_{0}^{\Delta t} \frac{\sigma^2(\Delta t - \tau)}{\Delta t} e^{-j\omega\tau} d\tau \quad . \qquad (4.2.7)$$

This transform is a well-known result. (See for example reference [9] page 340.) For $S_n(\omega)$ one obtains:

$$S_n(\omega) = \frac{4\sigma^2 \sin^2(\omega\Delta t/2)}{\omega^2 \Delta t} \quad . \qquad (4.2.8)$$

This result is illustrated in figure 13.

The computer model was implemented with $\Delta t = .05$ and $\sigma^2 = 1.0$. This gives the power spectrum a peak amplitude of .05 and the first zero crossing at 125.5 radians.

4.3 The Lowpass Filter

The lowpass filter chosen was a fifth order Chebyshev filter with a 0.5 dB passband ripple. The 0.5 dB cutoff frequency was set at 1.0 radian. Thus, the power spectrum of the noise process previously described is essentially flat (the variation is less than one percent) with an amplitude of .05 across the passband of the filter.

The implementation of the filter was similar to an implementation which could be used on an analog computer. That is, the differential equation describing the filter was solved using five integrators in series. The transfer function realized, in terms of s-domain notation, was:

$$H_c(s) = \frac{1}{s^5 + b_4 s^4 + b_3 s^3 + b_2 s^2 + b_1 s + b_0} \quad . \qquad (4.3.1)$$

A block diagram of the method used is shown in figure 14. The coefficients, b_i , were taken from Weinberg [10]. A listing of the computer program generating the filtered noise is included as Appendix C.

The frequency domain characteristics of the filter, as implemented on the digital computer, were determined by passing

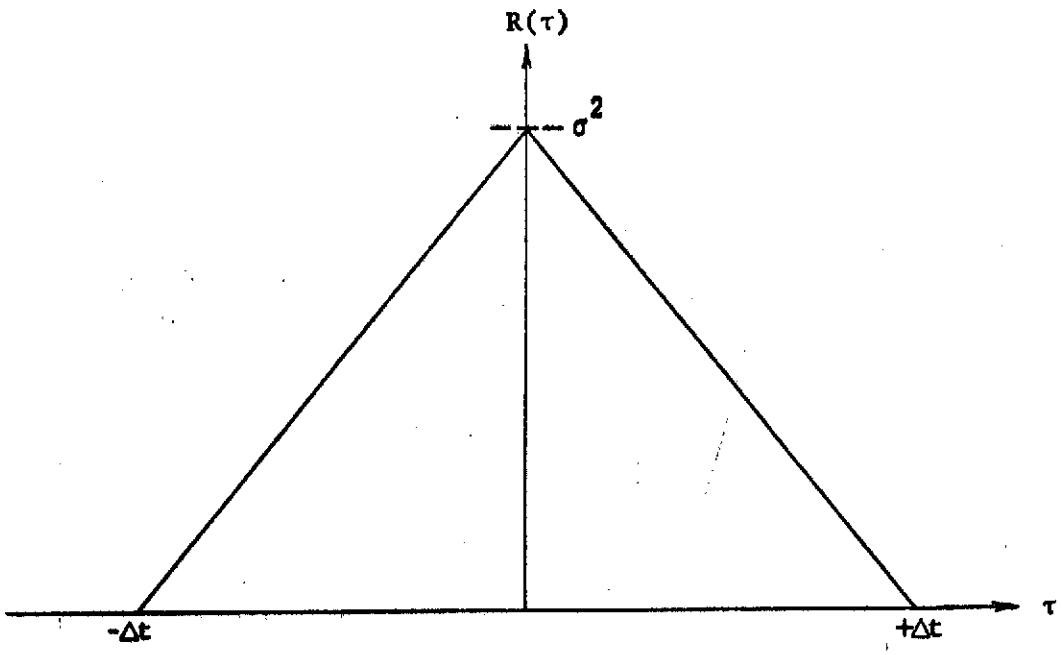

Wide-band Noise Autocorrelation Function

figure 12

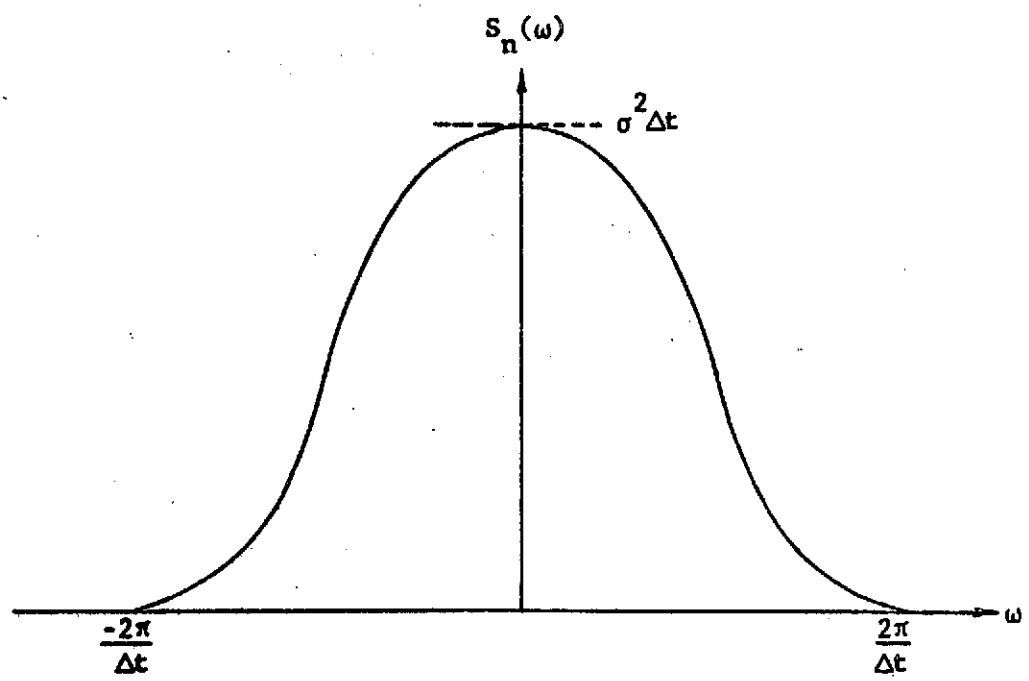

Wide-band Noise Power Spectrum

figure 13

sinusoids of known amplitude through the filter. The results of this test were found to be very close to that of an ideal Chebyshev filter. These results are plotted in figure 15. The plot is for a normalized filter.

There were many reasons for choosing this particular filter. The integration technique used was the same as that described in section 3.3. This was the highest order filter which could be easily implemented on the digital computer with this simple integration technique. It is sufficiently close to an ideal square filter to allow many analytical calculations to be done with this approximation. It is also very close to the characteristics of many IFs found in practical systems.

4.4 Empirical Verification of the Noise Model

This section describes tests made on the entire noise model which indicate that the previous analytical work, including assumptions, is valid.

The first test run was an estimation of the mean and variance of the output noise. This was accomplished by calculating the mean and variance of samples of the noise generated. For this test the output of the filter was multiplied by b_0 to give a normalized result.

The input process was generated with zero mean. Thus, the output of the linear filter should have zero mean. This was found to be consistently true, to within the accuracy of the digital computer, for samples of 2×10^5 points.

The variance of the output process can be calculated by assuming the input spectrum to be flat.

$$\sigma_0^2 = \tfrac{1}{2}\pi \int_{-\infty}^{\infty} S_0(\omega)d\omega \quad . \qquad (4.4.1)$$

$S_0(\omega)$ is the power spectrum of the output process. For a linear system:

$$S_0(\omega) = |H(j\omega)|^2 S_i(\omega) \quad . \qquad (4.4.2)$$

Thus, for this system:

$$\sigma_0^2 = \tfrac{1}{2}\pi \int_{-\infty}^{\infty} N_0/2 |H(j\omega)|^2 d\ \omega \quad . \qquad (4.4.3)$$

With the assumption of an ideal square filter of width one radian per second, the output variance becomes:

$$\sigma_0^2 = \tfrac{1}{2}\pi[N_0/2]\cdot 2 \quad . \qquad (4.4.4)$$

From the results of section 4.2:

$$\sigma_0^2 = .01590 \quad . \qquad (4.4.5)$$

The integral:

$$\tfrac{1}{2}\pi \int_{-\infty}^{\infty} |H(\omega)|^2 d\omega \qquad (4.4.6)$$

has been evaluated for a fifth order Chebyshev filter [11]. Using the tabulated value:

$$\sigma_0^2 = .01625 \qquad (4.4.7)$$

averaged over 4×10^5 sample points it was found that:

$$\sigma_0^2 = .01610 \quad . \qquad (4.4.8)$$

This is very good agreement.

Since the determination of the rate of impulses produced by a phase-lock loop tracking a carrier plus noise is an important objective of this work, the rate of impulses in the IF noise model is important. S. O. Rice [4] has developed a formula for this rate based on the radius of gyration of the noise:

$$R_R = r(1 - \text{erf}\sqrt{\rho}) \text{ impulses per second} \qquad (4.4.9)$$

where ρ is the numerical carrier to noise ratio and r is the radius of gyration of the noise. The $\text{erf}(x)$ is defined by:

$$\text{erf}(x) = [2/\sqrt{\pi}] \int_{-\infty}^{x} e^{-t^2} dt \quad . \qquad (4.4.10)$$

In order to better explain this calculation, a short digression on the definition of an IF impulse is in order. A phasor representation of the carrier plus noise is shown in figure 16. According to Rice's definition, an IF impulse occurs whenever the resultant phasor crosses the zero axis in the left half plane. The carrier amplitude in this model is set to $\sqrt{2}$. Thus, Rice's impulses are counted with this carrier amplitude.

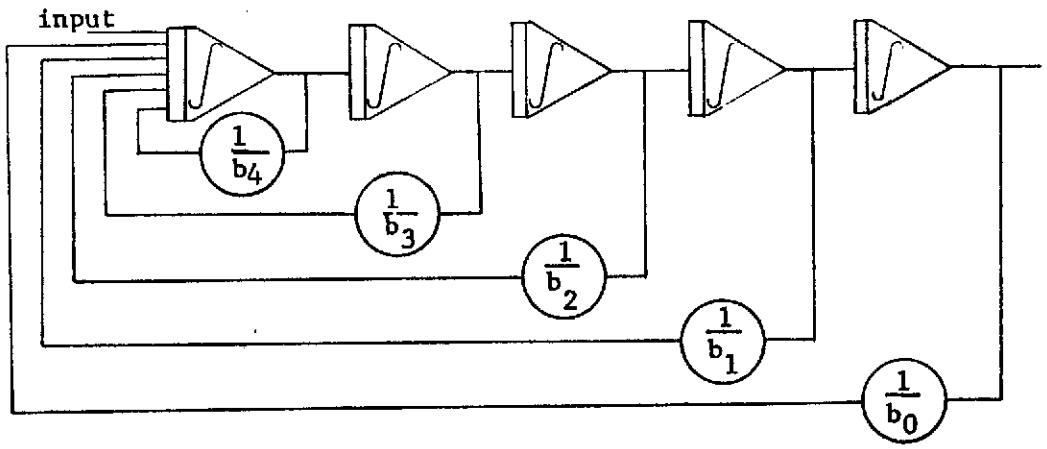

Block Diagram of Implementation of Noise Filter

figure 14

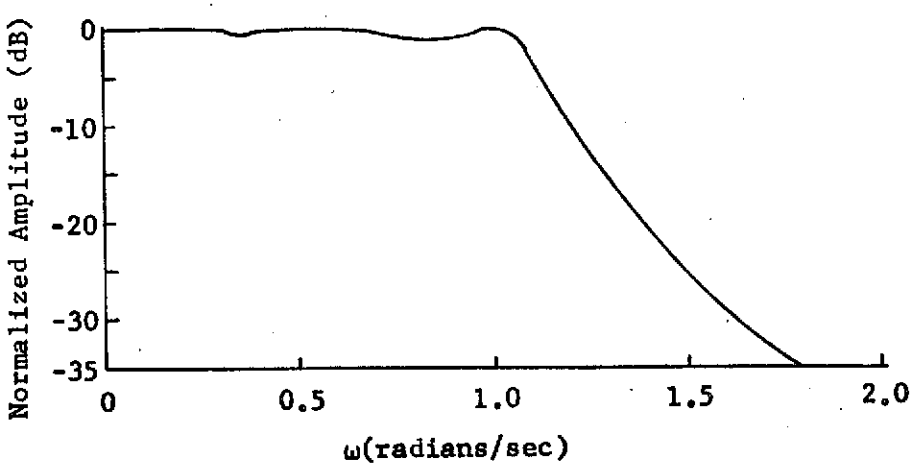

Transfer Function of 5^{th} Order Chebyshev Filter Simulated

figure 15

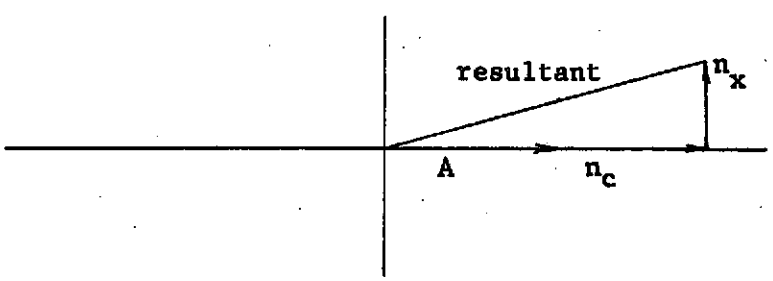

Phasor Diagram for IF Impulse Description

figure 16

Rice gives the radius of gyration of noise with an ideal square power spectrum as:

$$r_i = \beta/\sqrt{12} \qquad (4.4.11)$$

where β is the IF bandwidth. For an ideal square filter with a cutoff of one radian per second:

$$r_i = .0902 \quad . \qquad (4.4.12)$$

If the spectrum of the noise is assumed to be that produced by an ideal fifth order Chebyshev filter, the radius of gyration can be calculated:

$$r_c = .1525 \quad . \qquad (4.4.13)$$

This calculation is performed in Appendix D.

An empirical determination of the radius of gyration of the noise can be made by taking one-half the zero crossing rate of the quadrature component of the noise [4]. This estimate for the radius of gyration was made by observing the component for 4×10^4 seconds and gives an empirical radius of gyration of:

$$r_e = .1066 \quad . \qquad (4.4.14)$$

This indicates the variation of the filter, as implemented, from the ideal Chebyshev filter.

These rates and the rate observed during simulations are plotted versus carrier to noise ratio in figure 17. The IF impulse rate

observed during simulation is almost exactly that predicted with the empirically determined radius of gyration. Further, the rate predicted by the empirically determined radius of gyration lies above that predicted by an ideal square filter and below that predicted for the ideal Chebyshev filter.

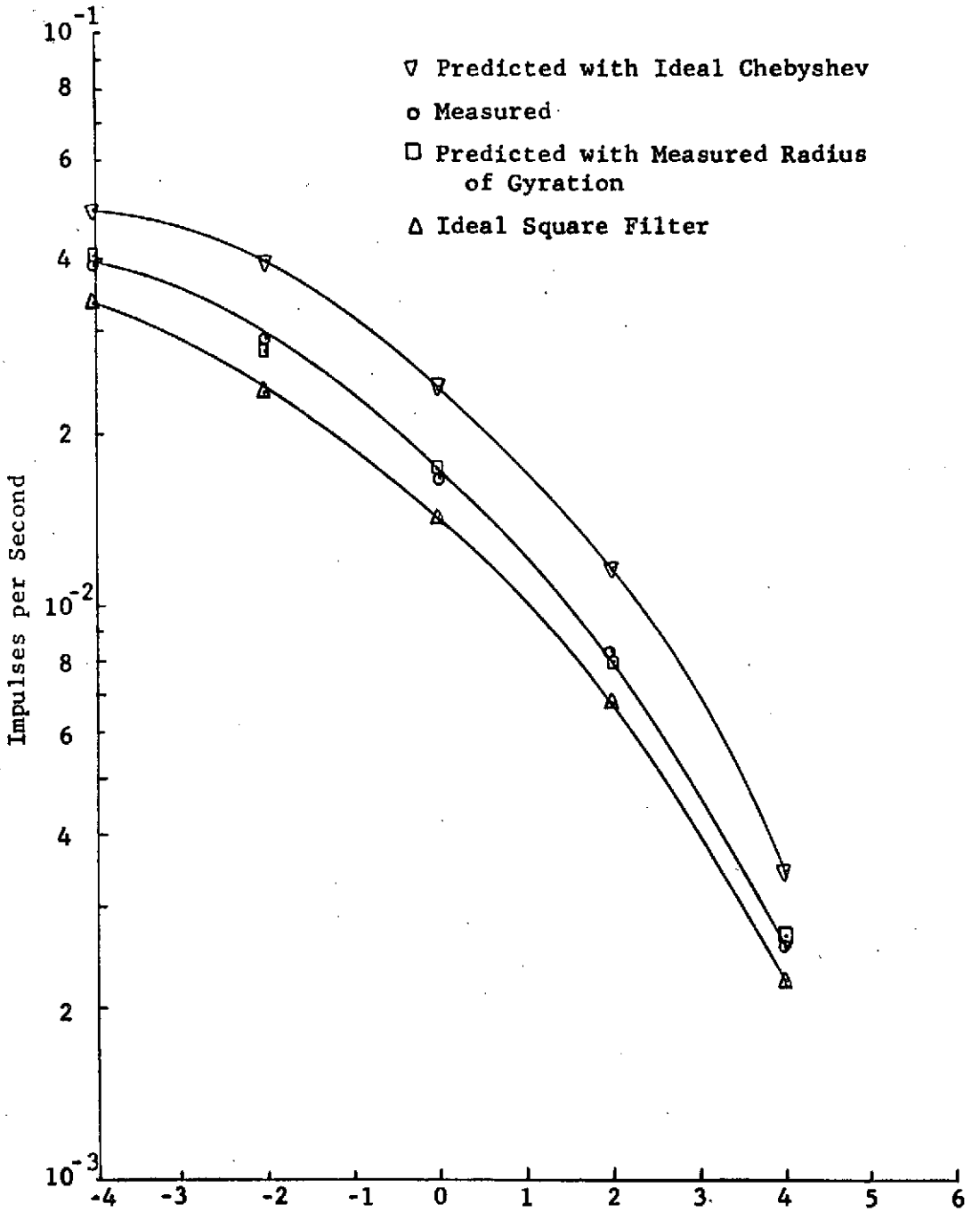

IF Impulse Rates

figure 17

CHAPTER V

THE GENERAL COMPUTER MODEL

5.1 Introduction

This chapter gives a detailed description of the digital computer implementation of the general PLL model developed in Chapter II. The method of inserting noise in the model is described. The method of determining the occurrence of PLL impulses and IF impulses is described. Section 5.4 presents cycle skipping rates (impulse rates) for the case in which the IF bandwidth is much greater than the PLL bandwidth and compares them to previously published results.

The relationship between loop carrier to noise ratio and output noise power is compared to recently obtained experimental results. Section 5.5 presents some new results obtained with the model presented in this thesis. These illustrate ways in which the model may be used.

The model was implemented in two phases. First, two time series of noise were generated on magnetic tape. Second, these noise processes were read into the PLL modeling program and used for $n_s(t)$ and $n_c(t)$ which are described in Chapter II. This approach was necessary because large amounts of time were required to generate the noise. A program was written which generated the noise it used internally. This approach was over 12 times as slow as the simulation using the noise from tape.

The noise processes, $n_s(t)$ and $n_c(t)$, are assumed independent in the derivation of the model. This was guaranteed in the computer model by the fact that the processes were generated in blocks of 2×10^5 points (see Appendix B). The last random number in the random number generator was saved at the end of each run and used to initialize the random number generator for the next run. The random numbers were independent of one another and thus the only correlation was that produced by the filter. The 2×10^5 points correspond to 10^4 seconds which is many times the decorrelation time of the filter. Thus, corresponding points in all of the time series are uncorrelated.

The same time series of noise from tape were used for many runs. The variations in carrier to noise ratio were obtained by multiplying the noise from tape by appropriate gain factors. The calculation of the gain factor is described in detail in section 5.2.

While the simulation was running, the test described in section 5.3 determined the occurrence of impulses in the IF noise. Section 5.4 describes the method used to detect PLL impulses. The time of occurrence of each IF impulse was printed as was the time of occurrence of each PLL impulse. The duration of each IF impulse was also part of the output. Finally, the total number of impulses of both types was summarized at the end of each run. The average noise power out of the PLL was also calculated for each run. The output format was such that additional information may be gleaned

from the data collected. This information is not directly applicable to the specific objective of this thesis.

A complete listing of the main simulation program is included in Appendix E.

5.2 The Gain Factor

A gain factor (called GAIN in the FORTRAN program) was used to adjust the amplitude of the noise time series to give the carrier to noise ratio desired in each simulation run. The components of this factor will be presented in three parts. First, there is an adjustment for the Chebyshev filter gain; second is the main portion of the factor which includes the carrier to noise ratio, and finally a factor of $\sqrt{1/2}$ introduced by the way in which the noise appears in the baseband model.

In the developmental stages of this work it was found that the simplest way to view the filter was as a normalized filter followed by an ideal amplifier. The noise generated on tape was the output of an unnormalized filter with gain, $1/b_0$. Thus, the first portion of the gain factor was b_0 which effectively normalized the filter.

In section 3.2, the model was specialized by setting the rms values of the carrier amplitude to one. Thus, the CNR (carrier to noise ratio in the IF) is simply the reciprocal of NP (noise power out of the fifth order Chebyshev filter).

$$CNR = 1/NP \quad . \tag{5.2.1}$$

The wide-band noise process has been shown to be flat across the passband of the filter with an amplitude in the passband of Δt . The noise power out of the filter is:

$$NP_0 = \frac{1}{2\pi}\int_{-\infty}^{\infty} S_0(\omega)\,d\omega \quad . \tag{5.2.2}$$

For a linear system with an input of white noise with spectral density, $N_0/2$, the output power spectrum is given by:

$$S_0(\omega) = [N_0/2]\ |H(j\omega)|^2 \quad . \tag{5.2.3}$$

Thus, substituting (5.2.3) in (5.2.2)

$$NP_0 = \frac{1}{2\pi}\int_{-\infty}^{\infty} \frac{N_0}{2}\, H(j\omega)H(-j\omega)d\omega \quad . \tag{5.2.4}$$

Now a change of variables, substituting s for $j\omega$, gives:

$$NP_0 = N_0/2 \left[\frac{1}{2\pi j}\int_{-j\infty}^{+j\infty} H(s)H(-s)ds\right] \tag{5.2.5}$$

where $H(s)$ is the s-domain transfer function of the filter. The integral in brackets (defined I_m for convenience) has been tabulated for a fifth order Chebyshev filter [11] .

$$I_m = 1.02/\pi \quad . \tag{5.2.6}$$

For convenience the approximation $1.02 \sim 1.0$ will be used. With this approximation, substituting (5.2.6) in (5.2.5) gives:

$$NP_0 = N_0/2\pi \quad . \tag{5.2.7}$$

Next, note that passing the output of the filter through an ideal amplifier with gain, G, will multiply the output power by G^2. Using such an amplifier in the model to provide the necessary amplitude changes gives:

$$NP = G^2 N_0/2\pi \quad . \tag{5.2.8}$$

Substituting (5.2.8) in (5.2.1) and solving for G gives:

$$G = \sqrt{20\ \pi/CNR} \quad . \tag{5.2.9}$$

This is the gain factor which would be needed on the output of a normalized filter to give a particular CNR.

Finally, from Chapter II, it can be seen that when the IF noise processes are $n_s(t)$ and $n_c(t)$, the noise processes in the phase-lock loop model are $\sqrt{\frac{1}{2}}\, n_s(t)$ and $\sqrt{\frac{1}{2}}\, n_c(t)$. Thus, the gain factor for the PLL model must be divided by the $\sqrt{2}$.

Combining the three factors just described gives the gain factor found in the PLL modeling program.

$$GAIN = .178923\sqrt{20\pi/2CNR} \quad . \tag{5.2.10}$$

In (5.2.10), .178923 is b_0 for the fifth order Chebyshev filter [10].

5.3 IF Impulse Detector

The definition of IF impulses has been described in detail in section 4.4. The most significant point to be brought out here is related to the gain factor previously calculated. The noise processes of the IF were divided by the $\sqrt{2}$ for input to the PLL model. It is much faster, in terms of computer time, to determine the IF impulses with the scaled version of the noise than to rescale the noise for this operation.

From the phasor diagram of figure 16 one can see that no IF impulse can occur while the amplitude of $n_c(t)$ is greater than the negative of the carrier amplitude. This condition was sensed by logic in the program. When this condition existed, each sign change of $n_s(t)$ was counted as an IF impulse.

In section 2.3 the carrier amplitude was fixed at $\sqrt{2}$. Thus, for an IF impulse to occur, the condition:

$$n_c(t) < -\sqrt{2} \qquad (5.3.1)$$

must exist. This condition implies that, in terms of the input noise processes for the PLL:

$$n_c(t)/\sqrt{2} < -1 \quad . \qquad (5.3.2)$$

This was the test used in the program logic. The sign changes of $n_s(t)$ are the same as those of $\sqrt{\frac{1}{2}}\, n_s(t)$. Thus, when the first condition was satisfied, the sign of the product of the current and previous points of $\sqrt{\frac{1}{2}}\, n_s(t)$ was tested. If the sign was negative,

an IF impulse was said to have occurred. One should note that the definition of an IF impulse used here is that given by Rice [4]. Other definitions have been used and could yield different results.

5.4 PLL Impulse Detector

PLL impulses were detected by observing a short term average of the output phase of the PLL. When comparing the results of this thesis with other work in the area, one should note that the output phase in this model is the negative of the difference in the phase of the VCO and the phase of the carrier. This result is obtained because carrier phase is set to zero in this model; that is, no modulation is present.

The differential equation describing the PLL, for no modulation present, has been shown to have stable points for an output phase of $\pm 2n\pi$ where $n = 0,1,2,3....$[3]. In the case with no modulation, the PLL produces an output impulse when the PLL moves from the vicinity of one stable point to another. This event requires a change in the average value of the output phase of 2π. The output of the PLL is the derivative of the output phase, and hence a level change in the output phase corresponds to an impulse at the PLL output.

In the early stages of the development of the model, the output phase was printed at each simulation interval. It was observed that whenever the long term average of the output phase changed by 2π, the change was very definite. Furthermore, the initial transient

occurring during the move from one stable point to another carried the output phase beyond the next stable point.

In the model presented in this thesis, the output phase was averaged over intervals two seconds long. Whenever this average was greater than 2π from the stable point around which the loop had been operating, the loop was said to have moved to a new stable point. This new value of $\pm 2n\pi$ was used for future comparisons. The two second averaging interval was chosen on the basis of the fact that, when the output phase was continuously printed, the output phase never went to a new stable point and stayed in that vicinity for this length of time and immediately returned to the original stable point. Qualitative analysis of the output phase points indicated that the changes from one stable point to another were sufficiently definite that the choice of the averaging interval was not critical.

5.5 Comparison with Other Results

The first results presented for comparison were originally presented in a paper by Sanneman and Rowbotham [2]. Through a computer simulation they determined the mean time to unlock for a PLL operating with carrier plus white noise as the input. Their result is given as a function of the CNR_L (carrier to noise ratio in the loop) in (5.5.1).

$$T_{ave} = [2/\omega_n]\exp \pi(CNR_L) \quad . \qquad (5.5.1)$$

The CNR_L was calculated using the equivalent noise bandwidth (B_L) for the linear baseband model of the PLL. This is derived by Viterbi [3].

$$B_L = \tfrac{1}{4}[2\zeta\omega_n + \omega_n/2\zeta]\text{Hz} \quad . \tag{5.5.2}$$

In order to achieve an effective approximation of white noise at the input to the PLL, ω_n of the loop was set at .1 and ζ was set to .707. This gives an equivalent noise bandwidth of .333 radians per second compared to a filter bandwidth of one radian per second.

To compare the results of the model developed in this thesis to those of Sanneman and Rowbotham, the mean time to unlock is converted to an average cycle skipping rate. This rate is then used to predict the number of impulses in the time intervals over which the thesis model was run. This comparison is shown in figure 18.

When comparing the results one must remember that the results from Sanneman and Rowbotham's work represent a mean time to unlock. Thus, if the loop skips two cycles in a relatively short time interval, this would correspond to unlocking only once. This bunching effect has been observed previously [12] and was observed with the model of this thesis. However, bunching does not begin to occur until several cycles are skipped. Further, the bunching effect increases as the CNR_L is decreased. Thus, for high values of CNR_L, one would expect the rates found by this model to agree

closely with that predicted using the mean time to unlock. At low values of CNR_L one would expect the rate given by the thesis model to be higher than that predicted using the mean time to unlock. In addition, one would expect the difference to increase as CNR_L decreases. All these results are apparent in figure 18.

A comment on the variation of the data is in order at this point. Computer runs were made in segments of 10^4 seconds each. The number plotted represents the average number of impulses in four such runs. The number of PLL impulses observed on individual runs varied by as much as a factor of four. This is, in part, due to the fact that, for an ω_n of one tenth, the decorrelation time of the loop is a significant fraction of the total simulation time. At high carrier to noise ratios this meant the number of impulses observed was not sufficient to obtain a reliable estimate of the impulse rate. At low carrier to noise ratios the bunching effect previously mentioned indicates all the impulses observed are not independent events. In this case, the run times were not long enough to give a number of independent events which would allow as accurate an estimate of the impulse rate as one might like. This accounts for the variance apparent in figure 18. Considering these factors, the agreement is very good.

A second comparison which supports the model is shown in figure 19. This is a comparison of the average noise power out of the loop

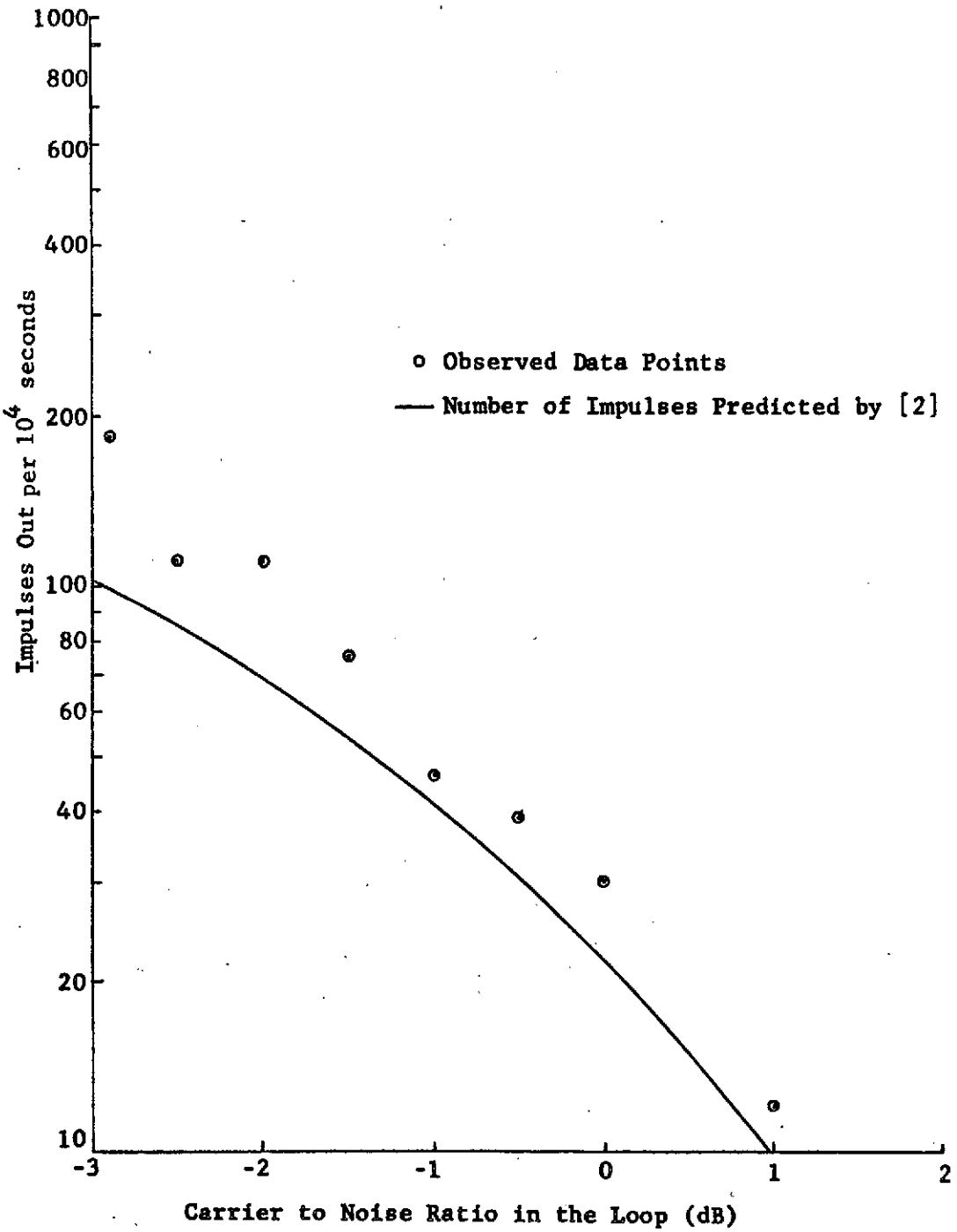

PLL Impulses for ω_n one tenth of IF Bandwidth

figure 18

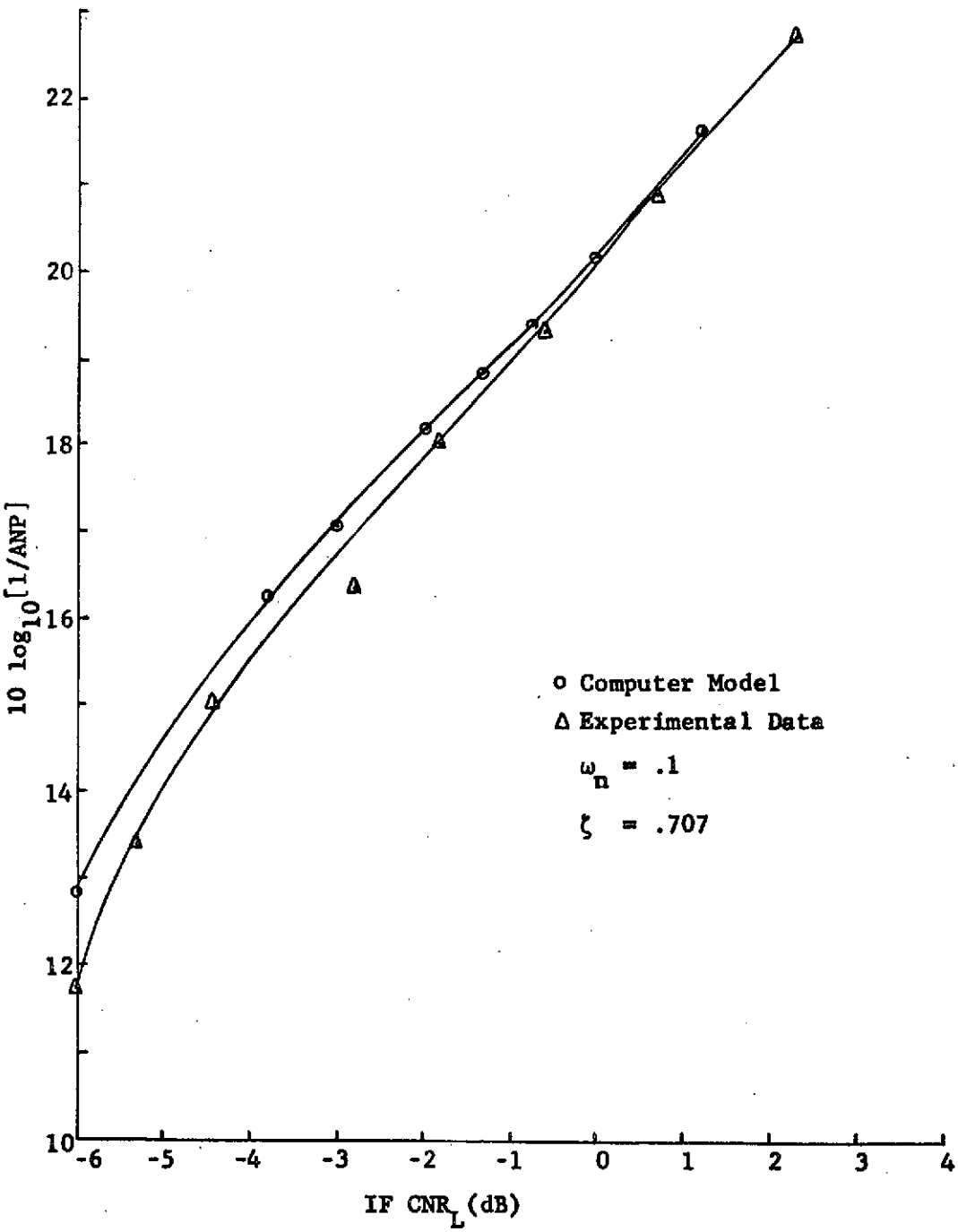

Output Noise Power vs. Carrier to Noise Ratio in the Loop
(ω_n Is One Tenth of IF Bandwidth)

figure 19

versus CNR_L with the same results obtained experimentally.* The experimental results are plotted with a constant offset. This is a result of differences in total noise powers. The significance of the curves is not in the exact values of output noise power, but in the fact that the shapes are almost the same. Further, the variations appear at low values of CNR_L. In this region accurate experimental measurements are very difficult to obtain.

5.6 New Results

This section presents results obtained with the computer model for ω_n of the PLL equal to the IF bandwidth. Figure 20 is a plot of the cycle skipping rate versus carrier to noise ratio in the IF. The CNR was used as the base parameter because the loop noise bandwidth is a meaningful parameter only when the white noise approximation at the input is valid. The results here were taken from two runs of 10^4 seconds for each point plotted. It was noted that the variation in the number of cycles skipped on each run was much smaller in this case than for the simulations run with ω_n of the PLL set to one tenth. The variation was generally on the order of one tenth the value shown. For a comparison, the PLL impulse rate predicted with Sanneman and Rowbotham's mean time to unlock is also plotted. This assumes the carrier to noise ratio in the loop

---

* The experimental results were obtained by A. Gilbert. They will be published in an upcoming report to the National Aeronautics and Space Administration under grant NGR-32-003-037. A similar curve is also given in reference [13].

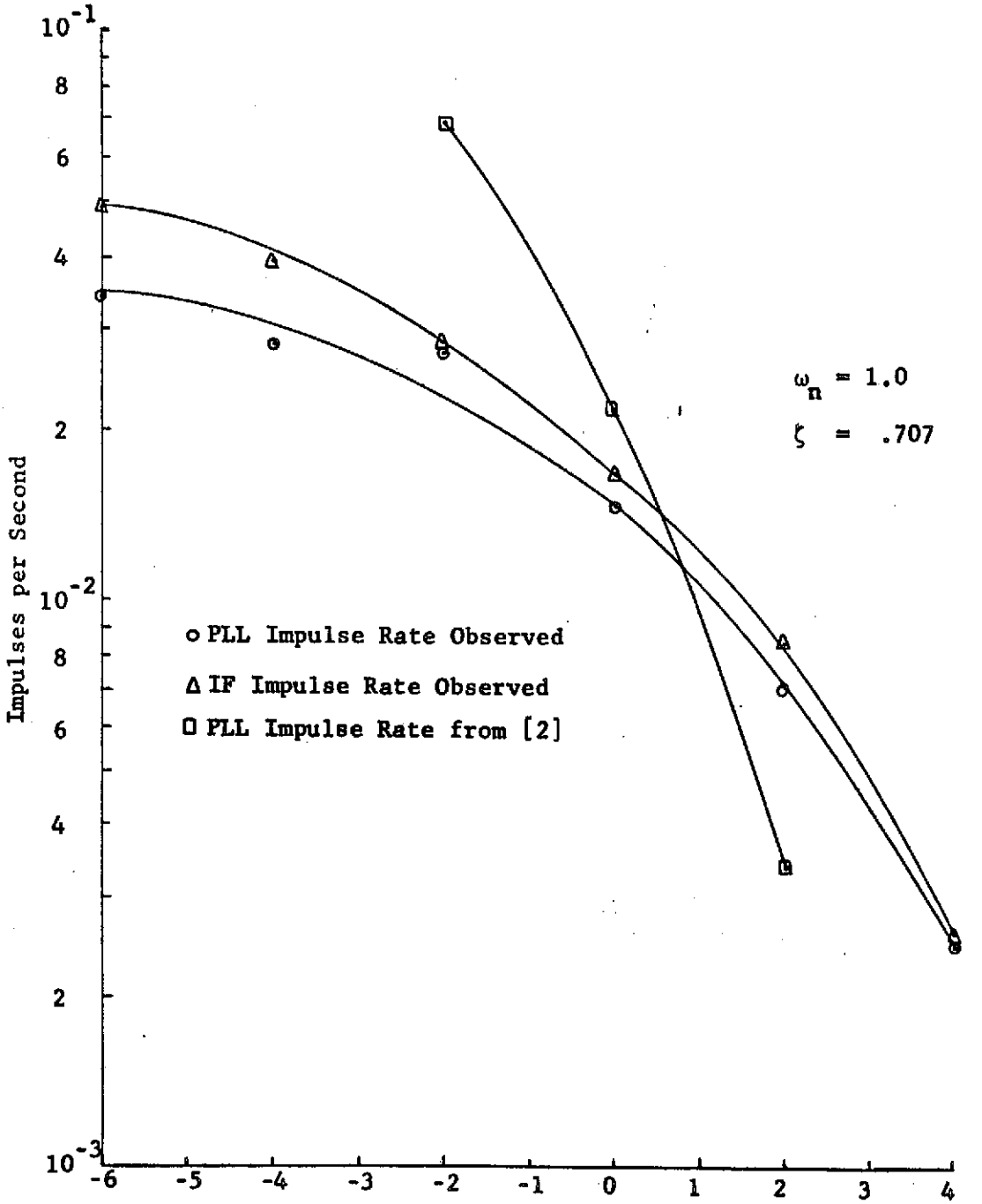

PLL Impulse Rate for ω_n Equal IF Bandwidth

figure 20

is equal to that in the IF. The rate of IF impulses observed, as defined by Rice, is also plotted on the same graph.

Figure 21 shows the effect on the number of PLL impulses of varying ζ with the IF bandwidth equal to ω_n of the PLL. Figure 22 shows the variation in average noise power out of the PLL for these same parameters. These results are of a preliminary nature and are included to illustrate the types of information that may be obtained with this model.

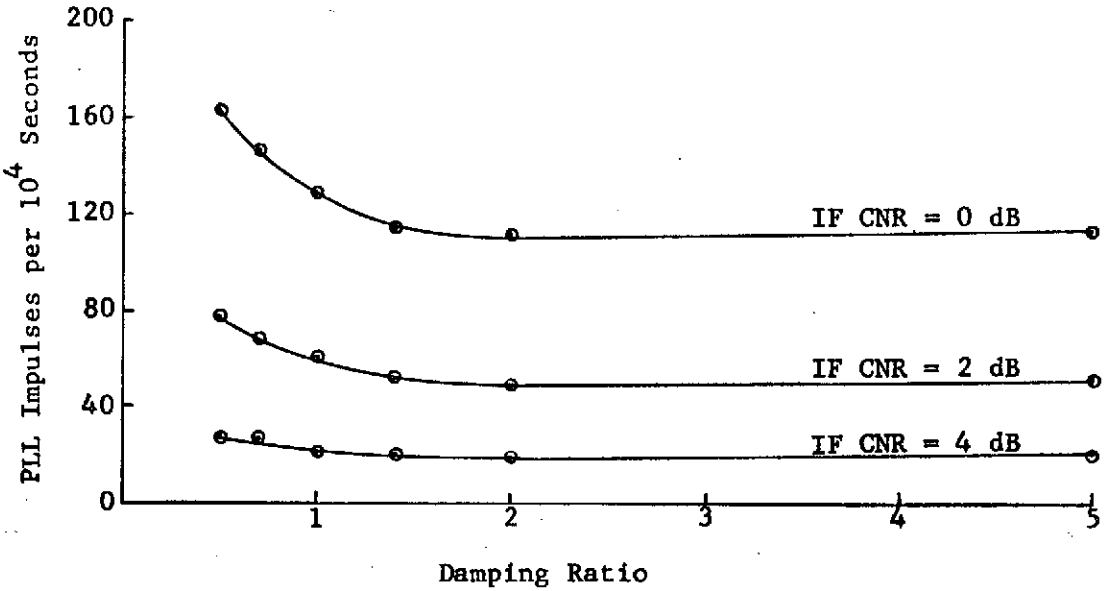

Variation in PLL Impulse Rate with Damping Ratio (for ω_n Equal IF Bandwidth)

figure 21

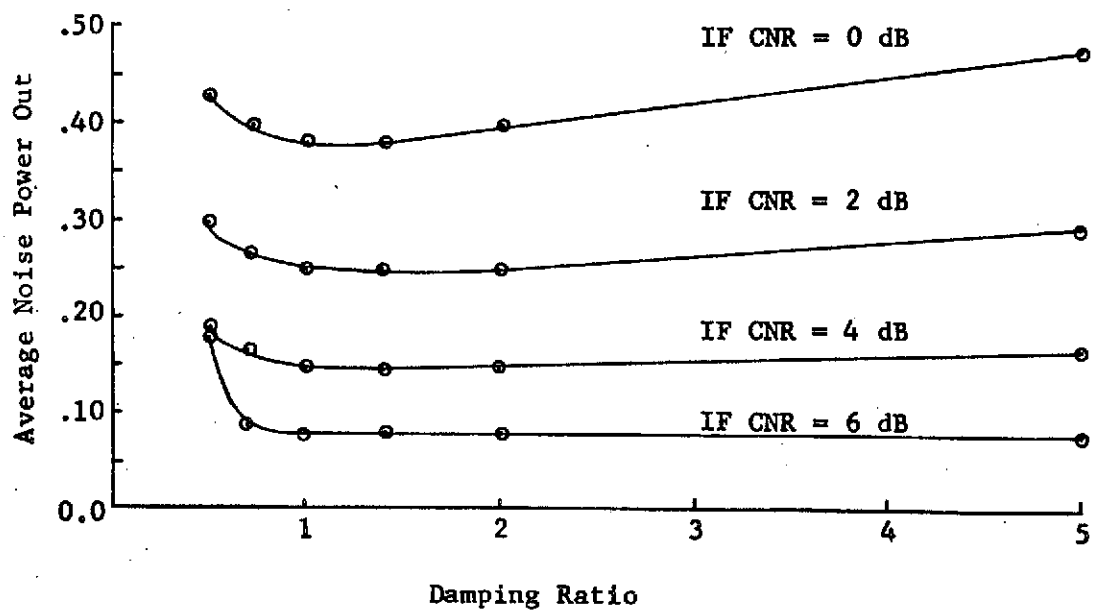

Variation in Output Noise Power with Damping Ratio (for ω_n Equal IF Bandwidth)

figure 22

CHAPTER VI

CONCLUSION AND RECOMMENDATIONS

6.1 Conclusion

The conclusion that may now be drawn is that a useful model of a second order PLL has been developed and verified. The model, as shown in this thesis, can provide data on performance of a second order PLL for a wide range of carrier to noise ratios and ratios of loop bandwidth to IF bandwidth. There are many areas in which this model is valid for which no analytical solutions predicting the performance of a second order PLL have been obtained. This is particularly important for the case where ω_n of the PLL is of the same order of magnitude as the IF bandwidth.

6.2 Recommendations for Future Study

Since the direct simulation approach used in this thesis has been shown to produce valid results, one area of future study would be a thorough study of the many numerical integration techniques to determine the method which will give the best trade off between machine computation time and accuracy.

As mentioned in Chapter V, there was some output from the computer runs which was not analyzed for the purposes of this thesis. This includes the duration of IF impulses and the times of occurrence of IF impulses and PLL impulses. Analysis of this data may allow a determination of a general relationship between IF impulses and PLL impulses.

As mentioned in the Introduction, only minor modifications would be required to add modulation to the model. This would simply involve structuring the main portion of the simulation in the manner shown in Chapter III. The desired output could be calculated and subtracted from the actual output to leave a measure of noise and distortion. It should be noted that the results presented in this thesis required approximately 15 hours of time on the IBM system 360 model 50. Each run of 10^4 seconds required from 4.5 to 5.5 minutes of computer time. The additional computations required for modulation could easily double this figure. Thus, detailed studies with modulation would require a faster computer. The problem is further complicated by the fact that the introduction of modulation increases the dimension of the parameter space of interest.

The extension to higher order loops is also straightforward. One may change the lowpass filter in the PLL to model any linear filter of reasonable order. The only restrictions are the accuracy of the computer and the computer time required.

CHAPTER VII

BIBLIOGRAPHY

[1] F. M. Gardner, Phaselock Techniques, John Wiley and Sons, Inc., New York, 1966.

[2] R. W. Sanneman and J. R. Rowbotham, "Unlock Characteristics of the Optimum Type II Phase-Locked Loop," IEEE Transactions on Aerospace and Navigational Electronics, Vol. ANE-11, pp. 15-24, March, 1964.

[3] A. J. Viterbi, Principles of Coherent Communications, McGraw-Hill, Inc., New York, 1966.

[4] S. O. Rice, "Noise in FM Receivers," Proceedings Symposium on Time Series Analysis, ed. M. Rosenblatt, Chapter 25, pp. 395-442, John Wiley and Sons, Inc., New York, 1963.

[5] F. E. Nixon, Principles of Automatic Control, Prentice-Hall, Inc., Englewood Cliffs, New Jersey, 1953.

[6] F. F. Carden, L. R. Kelly and T. B. Hintz, "The FM Demodulating Characteristics of Non-linear Phase-Locked Loops," Proceedings IEEE National Telemetry Conference, pp. 30-35, Houston (1968), IEEE Inc., New York, 1968.

[7] F. F. Carden, G. Lucky and G. Swinson, "The Quasi-stationary and Transient Behavior of Non-linear Phase-Lock Loops," SWIEECO Record of the Technical Program, Dallas, Texas, 1967.

[8] Y. F. Lee, Statistical Theory of Communication, John Wiley and Sons, Inc., New York, 1960.

[9] Athanasios Papoulis, Probability, Random Variables, and Stochastic Processes, McGraw-Hill, Inc., New York, 1965.

[10] Louis Weinberg, Network Analysis and Synthesis, McGraw-Hill, Inc., New York, 1962.

[11] L. G. Stolarczyk and W. P. Osborne, "Equivalent Noise Bandwidth of Electrical Wave Filters," Microwave Journal, to be published, 1970.

[12] F. J. Charles and W. C. Lindsey, "Some Analytical and Experimental Phase-Locked Loop Results for Low Signal-to-Noise Ratios," Proceedings of the IEEE, Vol. 59, No. 9, pp. 1152-1166, September, 1966.

[13] J. C. Lindenlaub and J. J. Uhran, "Threshold Study of Phase Lock Loop Systems," Technical Report No. TR-EE-66-19, Sponsored by National Aeronautics and Space Administration under Grant NSG-553, Lafayette, Indiana, December, 1966.

[14] System/360 Scientific Subroutine Package [360A-CM-03X] Version III Programmers Manual, International Business Machines Corporation, 1968.

[15] D. T. Hess, "Cycle Slipping in a First Order Phase-Locked Loop," IEEE Transactions on Communications Technology, Vol. COM-16, No. 2, pp. 255-260, IEEE Inc., New York, April, 1968.

[16] V. W. Eveleigh, Adaptive Control and Optimization Techniques, McGraw Hill, Inc., New York, 1967.

APPENDICES

APPENDIX A

COMPUTER PROGRAM FOR THE DETERMINISTIC MODEL

```
    DIMENSION A(1000),B(1000),Z(1000),C(1000)
    DO 100 JJ=1,20
    READ(5,2) ZETA,SS,WN
  2 FORMAT(3F10.5)
    WRITE(6,40) ZETA,SS,WN
 40 FORMAT('1ZETA=',F10.7,5X,'SS=',F10.7,5X,'WN=',F10.7)
    C1=2.0*ZETA*WN
    C2=WN*WN
    T=0.0
    TH0=0.0
    TH01=0.0
    TH00=0.0
    THOS0=0.0
    THOS20=0.0
    DO 20 I=1,1000
    DO 10 J=1,5
    T=T+.05
    THI=SS*T
    THE=THI-TH01
    TH1=SIN(THE)
    THOS11=C1*TH1
    THOS21=THOS20+C2*(TH1+TH0)*.025
    THOS1=THOS11+THOS21
    TH01=TH00+(THOS1+THOS0)*.025
    TH00=TH01
    THOS0=THOS1
    THOS20=THOS21
 10 TH0=TH1
    Z(I)=T
    C(I)=THOS1
    A(I)=TH01
 20 B(I)=THE
    WRITE(6,50) (A(I),B(I),Z(I),C(I),I=1,1000)
 50 FORMAT(1H ,4E20.10)
100 CONTINUE
    CALL EXIT
    END
```

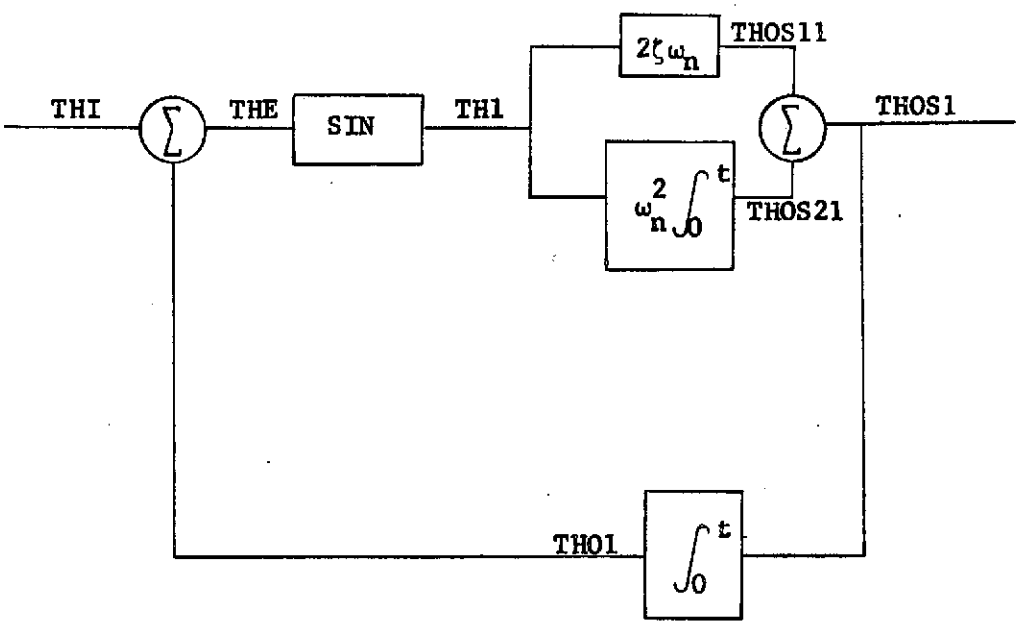

Block Diagram of Deterministic Model Annotated with Computer Program Variables

figure 23

APPENDIX B

THE RANDOM NUMBER GENERATOR

The program generating the gaussian numbers was obtained from the scientific subroutine package written for the computer used in this study. The subroutine which produced the normally distributed random numbers is called GAUSS. It utilizes another subroutine which generates uniformly distributed random numbers. This subroutine is called RANDU. Listings of GAUSS and RANDU, along with short descriptions, can be found in the manual for this package [14].

The general approach of GAUSS is to combine 12 uniformly distributed random numbers from RANDU to produce each normally distributed random number. This is significant because the uniform random number generator is a pseudorandom sequence generator. That is, it generates a finite sequence of random numbers and then repeats the sequence. If a subsequence of length less than the repetition length of the main sequence is subjected to statistical tests it will have all the statistical properties of a sequence of random numbers. The main sequence length with the subroutine used is 2^{29}.

Approximately 2×10^5 gaussian random numbers were used for each noise sequence generated for use in the model. This means 2.4×10^6 numbers were used from RANDU. However, 2^{29} is approximately 5.36×10^8. Thus, more than 200 such sequences could be generated before the basic random number generator repeats.

APPENDIX C

THE NOISE GENERATOR

```
    DIMENSION A(1000)
    READ(5,1)IX
  1 FORMAT(I10)
    B0=0.1789234
    B1=0.7525181
    B2=1.3095747
    B3=1.9373675
    B4=1.1724909
    Y5I=0.0
    Y4I=0.0
    Y3I=0.0
    Y2I=0.0
    Y1I=0.0
    Y0I=0.0
    DO 100 III=1,210
    DO 99 J=1,1000
    CALL GAUSS(IX,1.0,0.0,X)
    Y50=X-Y4I*B4-Y3I*B3-Y2I*B2-Y1I*B1-Y0I*B0
    Y40=Y4I+(Y50+Y5I)*.025
    Y30=Y3I+(Y40+Y4I)*.025
    Y20=Y2I+(Y30+Y3I)*.025
    Y10=Y1I+(Y20+Y2I)*.025
    Y00=Y0I+(Y10+Y1I)*.025
    Y5I=Y50
    Y4I=Y40
    Y3I=Y30
    Y2I=Y20
    Y1I=Y10
    Y0I=Y00
 99 A(J)=Y00
    WRITE (10) A
    IF(III.LT.10) GO TO 100
100 CONTINUE
    WRITE(6,2) IX
  2 FORMAT(1H ,I20)
    STOP
    END
```

APPENDIX D

RADIUS OF GYRATION OF NOISE FROM A FIFTH ORDER CHEBYSHEV FILTER

The radius of gyration, γ, of a narrow-band noise process is given by:

$$\gamma = \sqrt{\frac{\int_{-\infty}^{\infty} \omega^2 G(\omega) d\omega}{\int_{-\infty}^{\infty} G(\omega) d\omega}} \qquad (D.1)$$

where $G(\omega)$ is the lowpass equivalent power spectrum of the narrow-band noise [15]. For convenience, the integral in the numerator will be called I_1 and the integral in the denominator will be called I_2. The spectrum of the noise out of the Chebyshev filter used in this thesis is:

$$G(\omega) = [N_0/2]\,|H(j\omega)|^2 \qquad (D.2)$$

where $H(j\omega)$ is the transfer function of the Chebyshev filter.

Now I_1 will be calculated:

$$I_1 = N_0/2 \int_{-\infty}^{\infty} [j\omega H(j\omega)]\,[-j\omega H(-j\omega)]d\omega \; . \qquad (D.3)$$

Substituting s for $j\omega$, (D.3) can be rewritten as:

$$I_1 = [N_0/2] \cdot 2\pi \left[\frac{1}{2\pi j} \int_{-\omega}^{\omega} [sH(s)]\,[-sH(-s)]ds \right] \; . \qquad (D.4)$$

The integral in brackets has been tabulated in a general form [16]. Using the values for a fifth order Chebyshev filter one can obtain:

$$I_1 = (N_0/2)\cdot 4\pi^2(.0475) \quad . \tag{D.5}$$

The integral I_2 is simply the equivalent noise bandwidth for a fifth order Chebyshev filter. This is also tabulated [11]. From the tabulated value for $\omega_c = 1.0$:

$$I_2 = 2(N_0/2)(1.02) \quad . \tag{D.6}$$

Combining (D.5) and (D.6) one obtains:

$$\gamma = [2\pi\ (.0475/1.02)]^{\frac{1}{2}} \quad . \tag{D.7}$$

This gives a γ of .915. Rice's work was done in terms of frequency in cycles as opposed to the radian frequency shown here. Thus, the r for Rice's formula, shown in (4.4.13), is γ divided by 2π .

APPENDIX E

MAIN SIMULATION PROGRAM

```
      DIMENSION SS(1),XS(1000),SA(1),XC(1000)
      SS(1)=0.0
      SA(1)=0.0
C
C READ IN NUMBER OF SETS OF DATA
C
      READ(5,1)NDATA
    1 FORMAT(I5)
      DO 100 NNN=1,NDATA
C
C READ INPUT DATA FOR RUN
C
      READ(5,2)SN,WN,ZETA
    2 FORMAT(3F10.5)
C
C WRITE OUT DATA FOR RUN
C
      WRITE(6,3)SN,WN,ZETA
    3 FORMAT('1  SN='F10.5,5X'WN='F10.5,5X'ZETA='F10.5)
C
C COMPUTE GAIN TO GIVE DESIRED CARRIER TO NOISE RATIO
C
      ANP=0.0
      PI=3.1415927
      PIO2=PI/2.0
      GAIN=0.1789234*SQRT(20.0*PI/(SN*2.0))
C
C INITIALIZE VARIABLES
C
      NRI=0
      N=1
      NPLLP=0
      NPLLN=0
      NIMP=0
      NPLUS=0
      NMINUS=0
      MUE=0
      PI2=2.0*PI
      AVINT=0.0
      M=0
      T=0.0
      THO1=0.0
      THO0=0.0
```

```
      THOS0=0.0
      THOS20=0.0
      TH0=0.0
      C1=2.0*ZETA*WN
      C2=WN*WN
C
C START MAIN LOOP
C
      DO 98 J=1,200
      READ(10)XS
      READ(11)XC
      DO 50 L=1,1000
      XS(L)=XS(L)*GAIN
   50 XC(L)=XC(L)*GAIN
      DO 98 K=1,25
      DO 99 MM=1,40
      I=MM+(K-1)*40
      T=T+.05
      TH=-SIN(TH01)
      TH1=TH-XS(I)*TH+XC(I)*COS(TH01)
      THOS11=TH1*C1
      THOS21=THOS20+(TH0+TH1)*.025*C2
      THOS1=THOS11+THOS21
      TH01=TH00+(THOS1+THOS0)*.025
      TH00=TH01
      THOS0=THOS1
      THOS20=THOS21
      TH0=TH1
C
C MAIN PORTION OF SIMULATION ENDS
C BEGIN TESTS FOR CYCLE SKIPPING
C
      ANP=ANP+THOS1*THOS1*0.05
      AVINT=AVINT+TH01
   81 IF(XC(I).LT.-1.000) GO TO 83
      IF (M.NE.1)GO TO 99
      WRITE(6,6) M,N,TST,T
    6 FORMAT(3H M=,I5,5X,2HN=,I5,5X,4HTST=,E15.7,5X,2HT=,E15.7)
      IF(N.EQ.1) GO TO 87
      NIMP=NIMP+1
      IF(XS(I).GT.0.0) GO TO 86
      WRITE(6,200)
  200 FORMAT(' POSITIVE IF IMPULSE')
      NPLUS=NPLUS+1
      GO TO 87
   86 WRITE(6,300)
  300 FORMAT(' NEGATIVE IF IMPULSE')
      NMINUS=NMINUS+1
```

```
 87 N=1
    M=0
    TE=T-TST
    WRITE(6,7)TE
  7 FORMAT(' IMPULSE DURATION=',E15.7)
    GO TO 99
 83 IF(XS(I)*XS(I-1).GE.0.0) GO TO 84
    N=N*(-1)
    NRI=NRI+1
    WRITE (6,85)T
 85 FORMAT('0ZERO CROSSINGS'E15.7)
 84 IF(M.NE.1) TST=T
    M=1
 99 CONTINUE
    AVINT=AVINT/40.
    IF((MUE+1)*PI2.GT.AVINT) GO TO 90
    MUE=MUE+1
    NPLLP=NPLLP+1
    WRITE(6,91)T,AVINT
 91 FORMAT('0POSITIVE PLL IMPULSE AT',2E15.7/)
 90 IF((MUE-1)*PI2.LT.AVINT)GO TO 98
    MUE=MUE-1
    NPLLN=NPLLN+1
    WRITE(6,92)T,AVINT
 92 FORMAT('0NEGATIVE PLL IMPULSE AT',2E15.7/)
 98 AVINT=0.0
    WRITE(6,4000)NPLUS,NMINUS,NIMP,NPLLP,NPLLN
4000 FORMAT(' NPLUS=',I5,5X,'NMINUS=',I5,5X,'NIMP=',I5,5X,'NPLLP=',I5,5
   1X,'NPLLN=',I5)
    ANP=ANP/10000.0
    WRITE(6,4001)ANP
4001 FORMAT(' ANP=',E15.7)
    WRITE(6,4010) NRI
4010 FORMAT(' NUMBER OF RICE IMPULSES =',I 10)
    WRITE(6,9) NNN
  9 FORMAT(4H RUN,I2,2X,8HCOMPLETE)
    REWIND 10
    REWIND 11
100 CONTINUE
    CALL EXIT
    END
```